

Electronic Thesis and Dissertation Repository

8-13-2015 12:00 AM

Evaluation of Filtration Performance of a Rotating Belt Filter for Different Primary Wastewater Influent.

Tulip Chakraborty, *The University of Western Ontario*

Supervisor: Dr. Madhumita Ray, *The University of Western Ontario*

A thesis submitted in partial fulfillment of the requirements for the Master of Engineering Science degree in Chemical and Biochemical Engineering

© Tulip Chakraborty 2015

Follow this and additional works at: <https://ir.lib.uwo.ca/etd>

 Part of the [Biochemical and Biomolecular Engineering Commons](#), and the [Environmental Engineering Commons](#)

Recommended Citation

Chakraborty, Tulip, "Evaluation of Filtration Performance of a Rotating Belt Filter for Different Primary Wastewater Influent." (2015). *Electronic Thesis and Dissertation Repository*. 3165.
<https://ir.lib.uwo.ca/etd/3165>

This Dissertation/Thesis is brought to you for free and open access by Scholarship@Western. It has been accepted for inclusion in Electronic Thesis and Dissertation Repository by an authorized administrator of Scholarship@Western. For more information, please contact wlsadmin@uwo.ca.

EVALUATION OF FILTRATION PERFORMANCE OF A ROTATING BELT FILTER FOR DIFFERENT PRIMARY WASTEWATER INFLUENTS

(Thesis format: Monograph)

by

Tulip Chakraborty

Graduate program in Engineering Science

Department of Chemical and Biochemical Engineering

A thesis submitted in partial fulfillment

of the requirements for the degree of

Master of Engineering Science

The School of Graduate and Postdoctoral Studies

The University of Western Ontario

London, Ontario, Canada

© Tulip Chakraborty 2015

Abstract

Human activities around the world are responsible for production of enormous amount of wastewater, which needs to be treated quickly and effectively to avoid environmental concerns and other health implications. As an alternative to primary settlers in treating municipal wastewater, Salsnes, a subsidiary company of Trojan Technologies offers rotating belt filters (RBF) to treat the wastewater. A bench scale filtration unit of the RBF was developed to investigate the effect of varying water qualities from several wastewater plants in London, Ontario on the performance of the filter. The unit can achieve up to 80% reduction in total suspended solids (TSS), and 60% reduction in COD. As expected, flux of the filter meshes decreases with continuous filtration, while TSS, COD removal efficiency increases due to cake filtration. Performance models were developed correlating flux and removal efficiency with important influent water quality parameters such as TSS and COD using regression analysis.

Keywords: Cake filtration, Rotating Belt Filters, Regression analysis, Wastewater.

Acknowledgements

I would like to express my sincere gratitude to my supervisors Dr. Madhumita Ray and Dr. Amarjeet Bassi for their constant support and encouragement. Their constructive and useful criticisms towards my research studies helped and guided me improve my scientific viewpoint. Their availability at odd hours helped me overcome challenges with ease and comfort.

I appreciate and thank Trojan Technologies and MITACS for financial support. It has been a wonderful experience working with the Trojan Technologies research team as a whole. Thanks to Dr. Azita Soleymani and Dr. Domenico Santoro for being my constant guiding force at Trojan Technologies. Special thanks to Dr. Chris Degroot for all his help and support in helping me achieve my goals.

Special thanks to my family and my friends Souvarish Sarkar, Suvendu Indra, Suchismita Bose and Madhurima Roy for instilling the courage in me to go out and face the world and supporting me throughout my lab work and dissertation.

Dedication

This thesis is dedicated to the loving memory of my grandmother Sabitri Chakraborty.

Table of Contents

Abstract	ii
Acknowledgements	iii
Dedication	iv
List of Tables	viii
List of Figures	ix
List of Abbreviations	xi
List of Nomenclature	xii
Chapter 1	1
Introduction	1
1.1 Background:	1
1.2 Research objectives:	2
Chapter 2	3
Literature Review	3
2.1 Characteristics of wastewater:	3
2.2 Principles of existing techniques for measuring wastewater characteristics:	4
2.2.1 Total Suspended Solids (TSS):	4
2.2.2 Biochemical Oxygen Demand (BOD):	4
2.2.3 Total Organic Carbon (TOC):	5
2.2.4 Absorbance:	5

2.2.5 Turbidity:	6
2.2.6 Chemical Oxygen Demand (COD):	6
2.3 Filtration as a treatment method:.....	8
2.4 Different types of filtration:	10
2.4.1 Cake Filtration:	11
2.4.2 Dead-end filtration:.....	13
2.5 Concentration polarization:	14
2.6 Characterizing the filter mesh:	14
2.7 Modelling approach:	16
2.8 Future directions for the wastewater industry:.....	20
Chapter 3.....	21
Experimental.....	21
3.1.1 Collection of wastewater:.....	21
3.1.2 Development of a bench scale filter:.....	21
3.1.3 Calibrating the String Potentiometer:.....	23
3.1.4 Development of SOP for the column filtration test:	24
3.2 Analytical methods:.....	25
3.3 Statistical Software:.....	26
3.4 Regression Software:.....	27
Chapter 4.....	29

Results and Discussions	29
4.1 Variation in wastewater quality:	29
4.2 Characterizing the filter mesh:	31
4.3 First phase of data collection:	32
4.3.1 Building up the database:	33
4.3.2 Statistical analysis of the database:	40
4.4 Second phase of data collection:	46
4.4.1 Modified datasheet:	47
4.5 Regression analysis:	50
4.5.1 Validation of the flux model:	52
4.5.2 Validation of the removal efficiency model:	55
4.6 Response Surface Models:	59
Chapter 5	63
Conclusions:	63
5.1 Summary of results:	63
References:	65
Appendix:	86
Curriculum vitae:	80

List of Tables

2.1 Person load in various countries in kg/cap.yr	7
3.1 Specifications of the bench scale filter	22
4.1 Best 10 models predicted by AIC	41
4.2 Best 10 models predicted by BIC.....	41
4.3 Best 10 models predicted by Cp	42
4.4 Statistical analysis using SAS	43
4.5 JMP analysis	44
4.6 Modified kinetics datasheet	48
4.7 ANOVA analysis for removal efficiency	60

List of Figures

2.1 Range of spectral absorption	6
2.2 Different operations in a municipal wastewater plant	8
2.3 Formation of cake on a filter membrane	12
3.1 Schematic diagram of the column	23
3.2 Calibration of the string potentiometer	24
4.1 Variations in wastewater at the Pottersburg Pollution Control Plant	29
4.2 Changes in water quality at the Adelaide and Greenway Plants	30
4.3 Microscopic measurement of the 350 μm mesh	32
4.4 Microscopic measurement of the 158 μm mesh	32
4.5 Flux vs. TSS _a for the 350 μm mesh	34
4.6 Flux vs. TSS _a for the 158 μm mesh	35
4.7 Formation of cake on a filter mesh with TSS of 140mg/l.....	36
4.8 Formation of cake on a filter mesh with TSS of 265mg/l.....	36
4.9 Removal efficiency vs TSS _a for 350 μm mesh	37
4.10 Removal efficiency vs TSS _a for 158 μm mesh	37
4.11 COD vs. TSS _{effl} of the filtrate	38
4.12 Turbidity vs. TSS _{effl} of the filtrate	39
4.13 Turbidity vs. COD _{effl} of the filtrate	40
4.14 Actual vs. predicted flux as predicted by JMP	44
4.15 Analysis using HeuristicLab	45

4.16 Flowchart for the programming the modified datasheet	48
4.17 Regression tree obtained from H.L	51
4.18 Modelling flux vs. TSSa	52
4.19 H.L and Eureqa predicted values for flux	53
4.20 Validation of the flux model using random values	54
4.21 Regression tree obtained from H.L for removal efficiency.....	55
4.22 Observed vs. predicted values for removal efficiency	57
4.23 Removal efficiency model predicted by Eureqa	58
4.24 Removal efficiency model predicted by H.L	58
4.25 Surface plot of removal efficiency with TSSa and mesh	60

List of Abbreviations

Primary Influent (PI)

Total Suspended Solids (TSS)

Total Accumulated Suspended Solids (TSSa)

Chemical Oxygen Demand (COD)

Biochemical Oxygen Demand (BOD)

Concentration Polarization (CP)

Rotating Belt Filter (RBF)

Genetic Programming (GP)

HeuristicLab (H.L)

Response Surface Methodology (RSM)

Akaike Information Criterion (AIC)

Bayesian Information Criterion (BIC)

Jump (JMP)

List of Nomenclature

Q = Flowrate

Q_{in} = influent flow

A = Cross-sectional area of the filter

Δp = applied pressure differential across entire cake

r_i^* = inverse flux of layer i

L_i = depth of layer i

L = Total cake length = $\sum L_i$

μ = dynamic viscosity

k = average flux of cake

C_{in} = influent solids concentration

C_{out} = effluent solids concentration

ω = rotational speed of the screen

R_m = resistance due to screen

α = specific cake resistance

H = average water level

H_o = initial water level.

H_{ref} = water level in the effluent tank

ρ_w = water density at standard conditions

B = width of the screen

g = acceleration due to gravity

θ = angle of the filter

Chapter 1

Introduction

1.1 Background:

Human activities worldwide in the form of domestic, agricultural, industrial have resulted in increased water pollution. The quality in terms of the amount of solids present in the polluted wastewater vary from place to place with the changes being reflective of lifestyles of people of the particular region, the frequency and amount of precipitation, infiltration along with many other factors. A common practice for pre-treatment of wastewater is using the process of coagulation and flocculation. The most widely used coagulants are alum, ferric chloride and polyaluminium chloride (PAC). However, using these coagulants not only produces large volumes of sludge but large tanks with high surface area are then required to create good settling conditions. In densely populated regions this can significantly add to the investment costs.

While primary clarifiers are the most widely used units to remove mostly particulate chemical oxygen demand (COD) and total suspended solids (TSS) prior to biological treatment, the rotating belt filter (RBF) technology offers a smaller-footprint alternative to large setting tanks. It also provides faster installation, reduced capital and operational costs and energy savings in the long run. Such filtration systems operate on the principle of thin-cake filtration, which allows the removal of solid particles up to three times smaller than the nominal pore size of the filter mesh. The speed of the rotating belt can be adjusted to balance the cake thickness between the solids removal rate and the hydraulic surface loading.

Salsnes, Norway, a subsidiary company of Trojan Technologies, London, Ontario offers a wide range of the RBF units, rated for 400 to 600 gpm depending on inlet TSS concentration. These

units have been tested for effective TSS removal up to 80% and biochemical oxygen demand (BOD) up to 20% and maybe a viable alternative to primary settlers.

1.2 Research objectives:

As a certain filtration unit under constant operating conditions responds differently to a variation in the water quality and the filtration mesh type, semi-empirical approaches were adopted in developing the earlier filtration models. This is to avoid the need to consider the complex interactions between particulate solids and the filter mesh at the micro scale simplifying the modelling approach. The semi-empirical approach defines the filtration kinetics as the decay of the filter flux and the increase of the removal efficiency as the cake is forming on the filter mesh. The overall objective of this thesis is to determine the filtration kinetics of a Salsnes rotating belt filtration (RBF) unit using a bench scale version and develop filtration predictive performance model applicable for RBF.

The specific objectives of this work are to:

- Develop a bench scale filter unit and experimental protocol that enable the determination of filtration kinetics.
- Analyze the experimental data using regression analysis to determine the key wastewater parameters influencing the filtration kinetics.
- Develop a model that relates the wastewater characteristics (e.g. TSS, turbidity etc.) to flux and removal efficiency of the filter.
- Use the developed filtration kinetics model within a numerical simulation tool to predict the hydraulic capacity and removal efficiency of a full scale RBF.

Chapter 2

Literature Review

2.1 Characteristics of wastewater:

Wastewater is defined as an amalgamation of water containing wastes discharged from residential buildings, industries, institutions etc. and may also include storm water, surface water run-off and ground water [Metcalf and Eddy, 2002]. The contaminants in the wastewater range from particulate and colloidal matters in the form of sand, clay etc.; dissolved organic matter in the form of synthetic and natural compounds; inorganic matter in the form of nitrite, nitrate, ammonium, phosphate, sulfate; different microbes; heavy metals like arsenic, cadmium, lead etc.; hazardous and persistent organics like polycyclic aromatic hydrocarbons (PAHs), pesticides, and volatile organic chemicals (VOCs) etc. [Henze, 2008]. The changes in water quality are reflective of the lifestyles of the population in that region, daily consumption, regulatory laws in practice and different environmental factors such as nature and frequency of precipitation and soil constituents. For instance the variation in daily or the yearly load per person in countries like India, USA, Egypt, and Brazil may form a good basis while illustrating this point [Henze *et al.*, 2002]. As the wastewater flows out from the residences, industries, and into the sewer channels finally to the wastewater plants, it undergoes physical, chemical and biological changes. These changes can be determined by measuring certain global parameters, namely; total suspended solids (TSS), biological oxygen demand (BOD), chemical oxygen demand (COD), total organic carbon (TOC), absorbance, and turbidity [Bourgeois *et al.*, 2001].

2.2 Principles of existing techniques for measuring wastewater characteristics:

There occurs a spatial and time dependent variability in the water characteristics and in order to measure these changes, standard analytical methods exist. This section deals with describing the most common tests in detail.

2.2.1 Total Suspended Solids (TSS):

The American Public Health Association, American Water Works Association, and the Water Pollution Control Federation (1995) lists TSS as an important factor in water analysis. It requires obtaining a predetermined volume of water from the original sample, while it is being continuously stirred by a magnetic stirrer. This water sample is then passed through a glass fiber filter which had been previously washed, dried at 103°C and weighed. The difference between the initial and the final weights of the filter determines the mass of the suspended solids and knowing the sample volume TSS concentration can be calculated. A possible disadvantage to this conventional method could be the predetermined sample volume might not be representative of the entire water sample in the absence of complete mixing.

2.2.2 Biochemical Oxygen Demand (BOD):

The 5-day BOD test is an empirical test to measure bio - reducing pollution in the water. It is essentially the amount of dissolved oxygen required for the complete oxidation of the biodegradable compounds present in the sample in 5 days. Such test gives an indication of the biodegradability of the waste and is thus an important test for characterizing wastewater [Guwy *et al.*, 1999].

A major limitation of this test is that it requires diluting the sample which might result in reducing the concentration of the substances in the sample along with microorganisms thus paving the way for lower kinetic rates [Logan. 1993]. Though the manometric method doesn't require dilution of the sample, it inhibits the oxidation of ammonia. The presence of heavy metals in the sample water can affect the BOD readings and this has been well documented [Ademorotti. 1985].

2.2.3 Total Organic Carbon (TOC):

TOC is defined as the amount of organic carbon present in the sample and is regarded as one of the most important measures for wastewater quality as it reflects both the organic and the inorganic carbon present in water. The procedure for conducting TOC is fairly simple using standard TOC analyzers. One of the limitations of this test is its inability to identify the biodegradable and the non-biodegradable components.

2.2.4 Absorbance:

The use of electromagnetic radiation especially UV-absorbance in wastewater is mostly utilized to check for the presence of certain contaminants or compounds and is typically measured using a spectrophotometer. Different components of water absorb radiation at different wavelengths, e.g., absorbance at 475 nm stands for the color of the sample [Pena *et al.*, 2003]. The absorbance at 600 nm stands for the de - colorization of the wastewater [Solpan *et al.*, 2003] [Arslan *et al.*, 2000]. The figure on spectral absorption (Fig. 2.1) shows the range of wavelengths corresponding to the particular properties of the water.

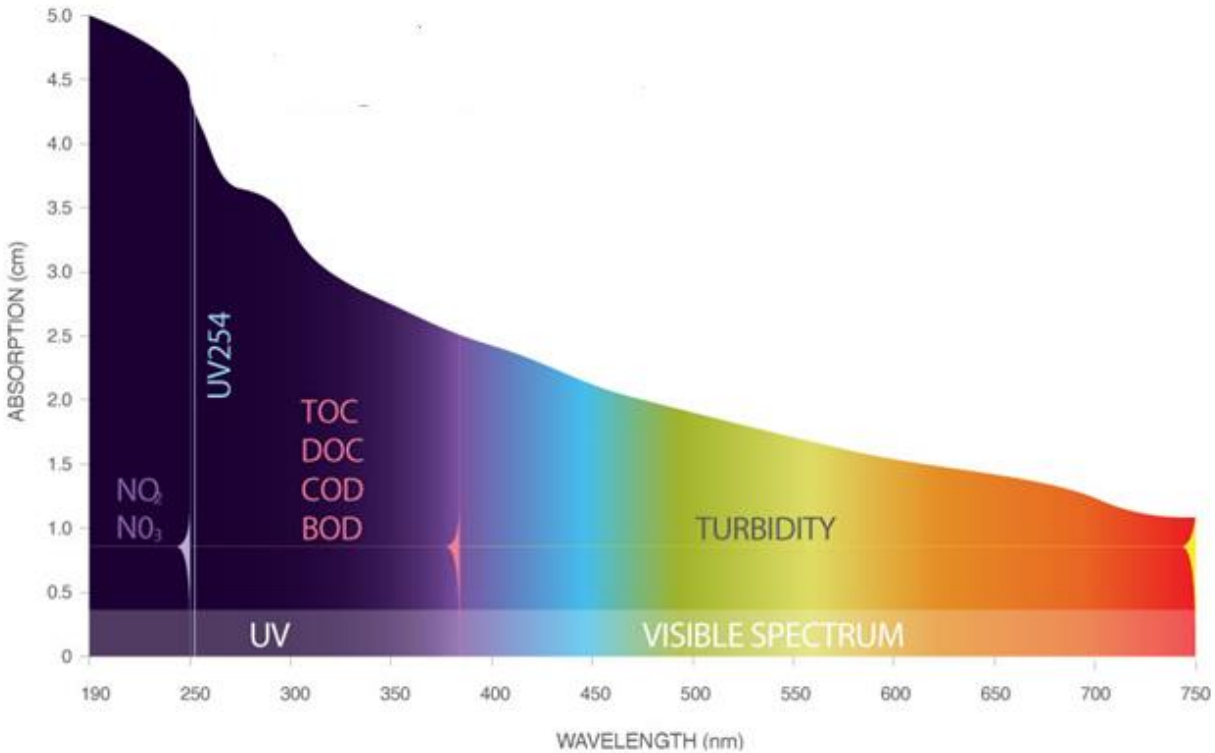


Fig 2.1: Range of spectral observation.

Adopted from <http://www.realtechwater.com/parameters/spectral-absorption>

2.2.5 Turbidity:

Turbidity is the measure of the clarity of the water. The amount of suspended and dissolved materials in the water gives an indication of the cloudiness of the sample. The procedure to measure turbidity is fairly simple with a turbidimeter, which works on the principle of light scattering by the particles in the sample at an angle of 90 degree to the incident beam. This is then related to the measurement of turbidity.

2.2.6 Chemical Oxygen Demand (COD):

Chemical oxygen demand is a measure of the amount of organic pollutants present in a water sample. It is widely used in wastewater industry as a fast and reliable method of determining the

quality of water after treatment. The principle behind COD is that all the organic compounds can be converted to carbon dioxide and water by chemical oxidation. It is measured as the amount of oxygen required to chemically oxidize all the organic pollutants in 1 liter (L) of water and is expressed as mg/L or ppm. Previously, COD was measured using a titration method with potassium dichromate, a strong oxidant. Other oxidants like KMnO_4 have also been used for measuring COD.

Though COD test has its own disadvantages like interference with chloride ions and also incomplete oxidation of several organic compounds it is still widely used as it is easy to perform and takes shorter time (1-3 hours) compared to BOD test (5 days) which takes much longer and requires expertise. Recently Li *et al.* (2009) introduced a method of measuring COD using a spectrophotometric method which has made COD measurement much faster and efficient.

As mentioned earlier, water quality varies significantly both temporally as well as geographically. Table 2.1 demonstrates such variations in important water quality parameters as discussed above.

Table 2.1: Person load in various countries in kg/cap.yr

Parameter	Brazil	Egypt	India	Turkey	US	Denmark	Germany
BOD	20-25	10-15	10-15	10-15	30-35	20-25	20-25
TSS	20-25	15-25		15-25	30-35	30-35	30-35
N total	3-5	3-5		3-5	5-7	5-7	4-6
P total	0.5-1	0.4-0.6		0.4-0.6	0.8-1.2	0.8-1.2	0.7-1

Adapted from biological wastewater treatment: principles, modelling and design by Henze M, Loosdrechst M, Ekama G. IWA publishing. 2008.

2.3 Filtration as a treatment method:

While the different characteristics of the water can be measured by examining TSS, BOD, COD and others, the wastewater generated needs to be treated in the most appropriate manner to ensure that the effluent concentrations meet the prevalent regulations. Typical wastewater treatment processes are shown in Fig 2.2. Economical pressure motivates the treatment companies to achieve such standards at lowest cost. Filtration as process intensification may be a possible alternative approach for primary treatment of wastewater, which removes most of the influent TSS and COD in a compact design.

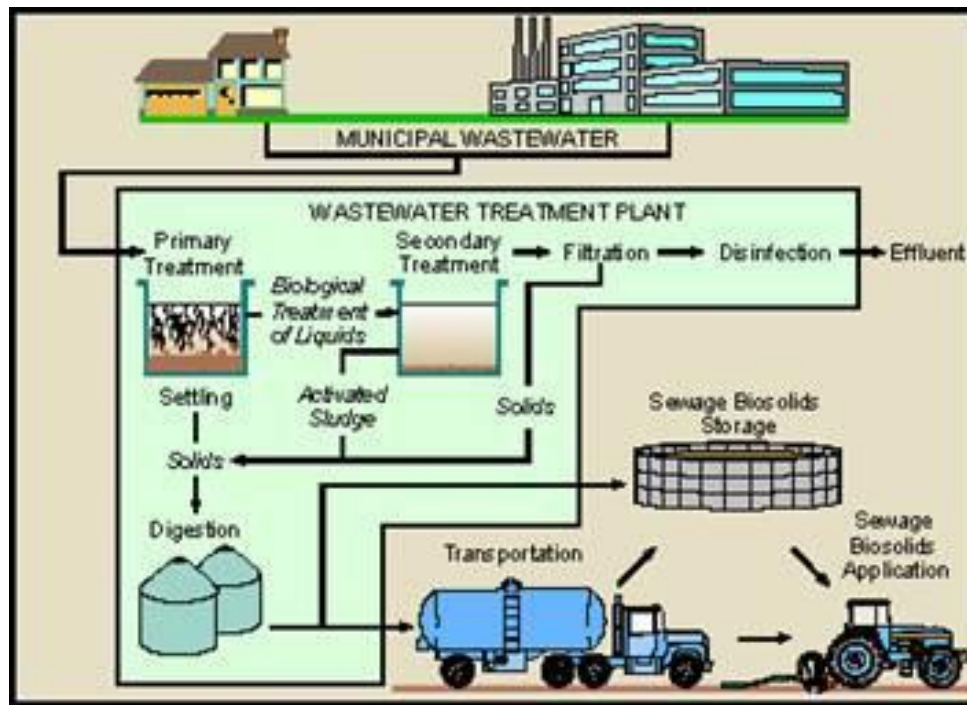


Fig 2.2: Different operations in a typical wastewater plant.

(Adapted from <http://www.omafra.gov.on.ca/english/nm/nasm/sewbiobroch.htm>; retrieved on

19/07/2015)

Filtration is defined as a process in which solids (particles) present in a suspension (mainly water) are separated from the liquid by forcing the flow of the suspension through a supported mesh or cloth. The products of this process consist of a nearly or particle-free fluid stream (filtrate), a solid phase with small amount of entrapped liquid and possibly a solid-fluid mixture [Tien. 2006]. Filtration not only finds applications in the wastewater industry but also in different process industries including pharmaceutical, chemical and dairy industries [Christy. 2002], [Saboya *et al.*, 2000] to name a few.

Although widely used in chemical and food processing industries, filtration in the wastewater industries is a relatively new concept as a primary treatment option. The first stage of treatment for wastewater entering the plant after screening is by coagulation – flocculation for settling the solids present in the water. The addition of a coagulant creates agglomeration of the nano to submicron colloidal particles to bigger particles resulting in quick sedimentation of the particles. When sedimentation is the primary process in wastewater treatment [Cristovao *et al.*, 2015] [Kadam *et al.*, 2015] [Sarkar *et al.*, 2006], settlers are needed to separate the solids from the water. The settlers can be either rectangular or circular. Due to slow settling rate, which is mainly due to the gravitational force, settlers require large volume occupying enormous space in the plant. Moreover the hydraulic loading capacity of these settlers is quite low and they fail to remove smaller suspended solids. These settlers not only occupy a huge amount of space in the plant but frequent sludge removal from the bottom is an issue.

The alternative technology to sedimentation is filtration which is capable to treat the raw water or the primary influent replacing primary sedimentation. RBF technology provides the alternative to sedimentation. The filter made of nylon mesh rotates like a conveyor belt and after each rotation; the filter mesh gets cleaned by water, or air jet. The cleaning procedures are

specific to each manufacturer and are patented. As the settling of the solids is a time consuming phenomenon, these units work instantaneously by impacting and intercepting the solids on the filter mesh.

Some of the filtration units such as Salsnes (acquired by Trojan Technologies, Inc.), Eco Mat RBF (Blue water Technologies), Hydrotech Beltfilters (Water management Technologies), etc, depending on their specifications can remove not only the TSS, but also reduce BOD, COD, and dewater sludge with their belt press. The land requirement for setting up these units is less than the space required for the settlers.

Salsnes, the filtration unit from Trojan Technologies works on the theory of cake filtration. The water enters through the inlet pipe and comes in contact with the filter mesh. The filter mesh inside the unit is set at an angle and rotates on its axis. The particulates in the water are trapped by the filter mesh and the filtrate passes through the pores. The filter mesh rotates and is cleaned using an air-knife. The particulates which have been cleaned from the mesh drops down to the sludge chamber, where it is dewatered and taken out of the system with an outlet pipe.

It is essential to know the filtration theory in detail before designing such units. The following sections provide an insight into the filtration process.

2.4 Different types of filtration:

The filtration process can be divided into the following categories:

- Cake filtration
 - Cross-flow filtration
 - Dead-end filtration

- Fabric filtration
- Vacuum filtration
- Deep bed filtration
 - Granular filtration
 - Cartridge filtration
 - Fibrous filtration

As this thesis is concerned with the formation of cake on the filter mesh, cake filtration technique has been investigated in greater depth

2.4.1 Cake Filtration:

When a solid suspension (slurry) is passed through a porous surface, the solids in the slurry are retained on the surface. As more of the slurry is passed through, the solids start building up on the mesh forming a thick cake like structure (Fig. 2.3). Formation of the cake on the membrane results in a higher removal efficiency of the feed stream as the thick mat formed traps particles within itself.

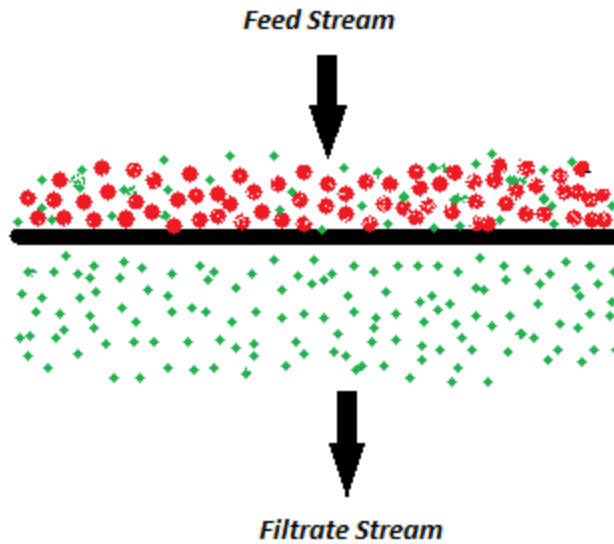


Fig. 2.3: Formation of cake on a filter membrane.

Models of cake filtration are developed following models of porous media including the most commonly used Darcy’s law. The result of Darcy’s classic experiments, globally known as Darcy’s law, states that: “the rate of flow Q of water through the filter bed is directly proportional to the area A of the sand and to the difference Δh in the height between the fluid heads at the inlet and outlet of the bed, and inversely proportional to the thickness L of the bed”.

This can be stated mathematically as:

$$Q = CA \frac{\Delta h}{L} \quad (2.1)$$

Where C is a property characteristic of the sand or porous media. Darcy’s law presents a linear relationship between the flow rate Q and the head (pressure gradient) $\Delta h/L$. The constant of proportionality C in the original Darcy equation has been expressed as k/μ , where μ is the viscosity of the fluid and k is called the permeability of the porous medium. Permeability is a property of the porous media and is independent of the nature of the fluid. The permeability k is

considered to completely and uniquely characterize the dynamic properties of a porous media with respect to flow of fluids through it.

Darcy's law can be rewritten as:

$$Q = \frac{kA}{\mu} \frac{dp}{dx} \quad (2.2)$$

Where $\frac{dp}{dx}$ is the pressure gradient.

2.4.2 Dead-end filtration:

In this kind of filtration the fluid stream is allowed to pass through the membrane and the particles larger than the pores of the membrane are trapped on it forming a cake [Perry. 2007]. The process can be pressure driven or gravity driven. In dead end filtration with the increasing process time, the retained particles keep building up over the membrane or within it. In either case, the particle building results in an increased resistance to filtration and causes the permeate flux to decline, as a result of which the process requires the stopping of filtration in order to clean or replace the membrane.

A commonly accepted fact for such filtration processes is that there is deposition of the particles as soon as the filtration process begins, resulting in the formation of a cake, but Petsev *et al.*, (1993) proved theoretically that when filtration of charged colloidal particles take place in the dead-end mode of filtration, agglomeration or coagulation of particles occurs at the membrane surface which is due to the fact that the hydrodynamic force acting on the first layer of particles at the membrane surface is much higher than the repulsive forces existing between particles caused by their charges.

2.5 Concentration polarization:

An important aspect of the filtration process is the phenomenon known as concentration polarization. Concentration polarization occurs when there is selective transfer of species across the membrane due to transmembrane driving forces [Hoek *et al.*, 2013] resulting in accumulation of the retained particulates. Concentration polarization is referred to the increase of concentration gradient of a particular substance close to a membrane solution interface due to the preferential flux of substances through the membrane. This phenomenon has been vastly studied in wastewater industry [Dunn *et al.*, 1987] [Ochando-Pulido *et al.*, 2015]. Due to the cake formation on the membrane surface, the pores are blocked by particle accumulation resulting in fouling. There are different mechanisms by which fouling can occur, namely by pore blocking, by adsorption, by concentration polarization and by cake formation [Belfort *et al.*, 1994]. All these ultimately resulting in change of the permeate flux [Bessiere *et al.*, 2005].

2.6 Characterizing the filter mesh:

The filter mesh plays a very important role in the process of filtration. It provides the surface required for the cake to form making it an essential component. There have been numerous studies on the use of fabrics or meshes as support material for the process of solid-liquid separation in wastewater treatment [Wang *et al.*, 2001]. One such study by Chu and Li (2006) stated that using the industrial cloth material, the permeate turbidity obtained was less than 9NTU (Nephelometric Turbidity Unit), and the major resistance was offered by the formation of the cake layer. Nylon meshes have been tested at lab scale for both municipal and synthetic wastewater to good effect [Wu *et al.*, 2003] [Wu *et al.*, 2005]. In addition to this, ceramic or inorganic membranes which are expensive offer better chemical and physical stabilities along

with longer lifespan [Tewari *et al.*, 2010]. Since these membranes are expensive, alternate options are required. Waste materials like fly-ash [Batra. 2006], Clay [Wang *et al.*, 2001] [Rakib *et al.*, 2001] and mixed oxides have been used to develop the ceramic membranes. Studies have shown that with cordierite as a support material [Saffaj *et al.*, 2004] and Moroccan clay [Saffaj *et al.*, 2005], the membranes can effectively reject heavy metals like Cr, Pb, Cd and dyes. Such alternatives have lowered the costs and the filtration resistances as offered by the microporous membranes [Li *et al.*, 2011] thus enabling lowering of replacement costs of the membranes and operating costs using efficient gravity driven filtration [Satyawali. 2008].

However for mesh filters, the deposition of particulate matter resulting in the formation of a cake is intentional and is critical in the separation of the solid-liquid mixture [Chu. 2006]. This cake can be formed, cleaned, and reformed again during the entire process of filtration [Seo *et al.*, 2007]. For the cake to form on the mesh surface, it is essential to first characterize the filter mesh. Characterization of the filter mesh can be achieved by different methods, namely:

- SEM (Scanning Electron Microscopy)
- TEM (Transmission Electron Microscopy)
- Porosimetry

SEM and TEM find uses in a number of fields like wastewater research [Zhou *et al.*, 2015], biology [Lawrence *et al.*, 2003], bio-process engineering [Diaz *et al.*, 2006] [Baloch *et al.*, 2008]. Porosimetry has been used to accurately measure the pore size in a filter mesh. Several companies while manufacturing filter meshes state the nominal pore size of the mesh, however, for research it is important to know the actual pore size, which is measured by porosimetry. Porosimetry has been used to characterize resin [Monteagudo *et al.*, 2000],

catalyst [Qin *et al.*, 2011], enzymes [Mesquita *et al.*, 2012] [Zhang *et al.*, 2012], [Sanchez-Martin *et al.*, 2013].

2.7 Modelling approach:

In the past 40 years [Belia *et al.*, 2009] there has been substantial development when it comes to wastewater engineering and the knowledge gain from this has been phenomenal. This acquired sense of knowledge has resulted in construction of numerous mathematical models which on validation have deepened the understanding in the wastewater field. In the last few decades, the use of mathematical or statistical models, have been classified as the appropriate means to gain an extensive insight into environmental management problems thus providing valuable information [Poch *et al.*, 2004]. These constructed models have been used on validating numerous datasets to good extent.

There are a number of algorithms and the major ones are genetic programming [Koza, 1992], evolutionary strategies [Fogel *et al.*, 1996], evolutionary programming [Rechenberg. 1973], and genetic algorithms [Holland. 1975] [Goldberg. 1989]. Each of the above mentioned algorithms follow a distinct approach; however, they all are embedded with the same principles of natural evolution in genes.

Symbolic regression which belongs to a class of genetic programming [Koza, 1992] deals with induced models which are then restricted to mathematical functions. Conventional regression analysis involves assuming a model form and then determining the parameters which make that assumed model fit the observed data best. The advantage of symbolic regression over standard regression methods is that in symbolic regression, the search process works simultaneously on both the model specification problem and the problem of fitting coefficients. Symbolic regression would thus appear to be a particularly valuable tool for the analysis of experimental

data [Duffy. 2002]. The commercial software doing this kind of regression analysis would be HeuristicLab, Eureka etc.

Statistical modeling software such as statistical analysis software (SAS), JMP, ModeFrontier, Minitab and numerous others have created their own benchmarks. These software are based on different criteria for model such as Akaike Information Criterion (AIC), Bayesian Information criterion (BIC) and Cp as the criteria for goodness of fit. Depending on the user's need, the software can be run using its in-built programs and codes or the user could code to obtain the best results.

Development of models in unit operations like filtration provides insight of the interactions of a wide range of wastewater characteristics and the different operating parameters. Rigorous process models not only help in understanding the process, but also provide decisive characteristics in order to enhance operational strategies [Broeckmann *et al.*, 2006]. As this thesis deals mostly with cake filtration, the discussion is mostly limited to such models.

Darcy's law is perhaps the most fundamental theory when it comes to filtration. It has led to several other complicated equations and theories. Researchers in their works have advocated in giving time for a thin cake formation by gravity drainage prior to application of the pressure differential [Christensen and Dick (1985a, 1985b)] [Vesilind.1979]. This theory was then verified by Wells and Dick (1988) who in their work evaluated the impact of the cake formation period with respect to the computed specific resistances.

Greenkorn (1982) considered Darcy's law to be written for fluid flow through a number of cake layers or different flux as:

$$Q = \frac{A\Delta p}{\mu \sum r_i * L_i} = \frac{A\Delta p}{\mu \sum \frac{L_i}{K_i}} = \frac{kA\Delta p}{\mu L} \quad (2.3)$$

Where Q: flowrate through cake

A: Cross-sectional area of the filtration cell

Δp : applied pressure differential across entire cake

r_i^* : inverse flux of layer i

L_i : depth of layer i

μ : dynamic viscosity

L: Total cake length = $\sum L_i$

k: average flux of cake

For gravity filtration, the pressure differential and the cake length are function of time, and thus the Darcy's Law can be modified to be written as:

$$Q = \frac{kA}{\mu} \frac{\Delta p(t)}{L(t)} = \frac{kA}{\mu} \frac{\rho gh(t)}{L(t)} \quad (2.4)$$

Where h is the distance from top of the cake to the free water surface. Average flux calculation has been used in this thesis where the pressure has been assumed to linearly vary with the height of the column.

Using mass balance and modified Darcy's law, RBF's are modeled. Aarts *et al.* (2014) describes the modeling approach of a rotating fine screen filter. These screens offer much smaller footprint for treating different types of wastewater. The study was concerned at developing a physical fine screen model which would help in understanding the interaction between the solids removal rate, the broad range of wastewater characteristics along with the operational parameters. The model at steady state conditions can be written as:

$$C_{in} - C_{out} = \frac{\omega \cdot B}{Q_{in} \cdot \alpha} \left(\frac{B \cdot g \cdot \rho_w \cdot (H - H_{ref}) \cdot H_0}{Q_{in} \cdot \mu \cdot \sin \theta} - R_M \right) \quad (2.5)$$

Where C_{in} and C_{out} are the influent and effluent solids concentration

Q_{in} = influent flow

ω = rotational speed of the screen

R_m = resistance due to screen

μ = viscosity of the effluent

α = specific cake resistance

H = average water level

H_0 = initial water level.

H_{ref} = water level in the effluent tank

ρ_w = water density at standard conditions

B = width of the screen

g = acceleration due to gravity

θ = angle of the filter

Ho and Zydney (2000) developed a general model for both pore blockage and cake filtration stages along with the transition stages. The model developed by them provided an insight into the initial fouling caused by pore blockage and subsequent fouling resulting in deposition of cake over the initially blocked pores. Another model by Astarac *et al.*, (2014) which was developed similar to the model created by Ho and Zydney (2000) stated that the rate of fouling in hydrophilic membranes with smaller water contact angle was much smaller than that in hydrophobic membranes with larger water contact angle. Jorgensen *et al.*, (2014) indicated that

the cake layer removal from the membrane surface followed the same kinetics as deposition of cake layer.

All of these models or in general most of the models are fitted with real time data collected from actual experiments to check accuracy of prediction. Such models not only play a crucial role in determining the direction of operation but also provide a glimpse to the complex interactions occurring within the unit processes.

2.8 Future directions for the wastewater industry:

Most of the wastewater plants in Canada were built during the 1950's and the estimated productive life of the wastewater treatment assets have passed 63% in 2007 [Statistics Canada, Govt. of Canada]. Given this scenario in the wastewater management, innovation needs to be the key for future growth and sustainability. With the growing concern on economic and environmental footprints, every treatment process in traditional wastewater treatment plants needs to be revisited. To achieve this, every treatment step for wastewater treatment has to be reevaluated be it primary, secondary or tertiary. The Salsnes filters with RBF technology could be a possible option in the primary treatment. Optimization of the filtration unit with external addition of probes for instantaneous measurement of water characteristics could go a long way in predicting the filtration kinetics in a particular geographical region. Developing a process model based on the relevant water characteristics unique to different geographical regions would enable catering the needs of wider users in wastewater management. This thesis aims to provide a model to predict the filtration kinetics of different wastewater characteristics using a bench scale unit of the Salsnes filter.

Chapter 3

Experimental

3.1.1 Collection of wastewater:

The city of London, Ontario has six wastewater treatment plants located across the city to treat the municipal wastewater. The six wastewater plants are located at Vauxhall, Oxford, Greenway, Pottersburg, Adelaide, and Southland with 36 pumping stations across the city. These plants employ all the necessary wastewater treatment steps before disinfecting the water with UV and releasing it to the Thames River. Wastewater samples for all the experiments were collected from the three main plants mainly Pottersburg, Greenway and Adelaide pollution control plants. The experiments were conducted during the months of January – June 2015, which included days after snowfall or heavy rain. Once the filtered water was collected, they were brought back to the Trojan Technologies lab for post processing.

3.1.2 Development of a bench scale filter:

A bench scale filter was setup to mimic the hydraulic height of the full scale Salsnes filtration unit located at Pottersburg pollution control plant. Since the Salsnes unit could not be moved from one plant to the other, the bench scale was used to serve this purpose. As mentioned, only the hydraulic height of the Salsnes was only mimicked, the cleaning procedure or the rotating belt filter could not be brought into the column setup. The bench scale unit comprised of a column with an adjustable valve connected to a string potentiometer to calculate the instantaneous water level. The string potentiometer functions by detecting, measuring position and velocity of the float attached with it using a flexible cable, a spring-loaded spool, and a rotational sensor. With the body of the potentiometer fixed to a surface and the stainless steel cable attached to a movable object (in this case, a float), the device produces an electrical signal

that is proportional to the cable's extension or velocity. This signal can be sent to a data acquisition system and finally to a computer from where the water level can be read. The string potentiometer was calibrated by measuring the voltages at different heights and a macros-enabled excel sheet was developed to calculate the height from the voltage instantaneously. At the very end of the column, just above the valve, the filter mesh was mounted. To avoid excessive spilling, a proper drainage system was devised using a hose and sample bottles for collection of the filtered water. The design specifications (Table 3.1) and the schematic diagram of the column (Figure 3.1) have been given below.

Table 3.1: Specifications of the bench scale filter

Actual column height, L (m)	1.22
[Manufactured by Plastco; NPS 2]	
Initial water level read on tape measure, h (m)	1.22
Origin of tape measure	Bottom of the column
Diameter of filtration area, Dm (cm)	4.849
Inner diameter of the column, IDc (cm)	5.08
Empty space depth between valve and filter, X (cm)	8.731
Length of hose (cm)	22.86
String Potentiometer	SP2-50
[Manufactured by Intertechnology Inc.]	
Length of float (cm)	9.1
Weight of the float (g)	310
Filter mesh size (\square m)	350, 158
Sample volume (mL)	2000.00

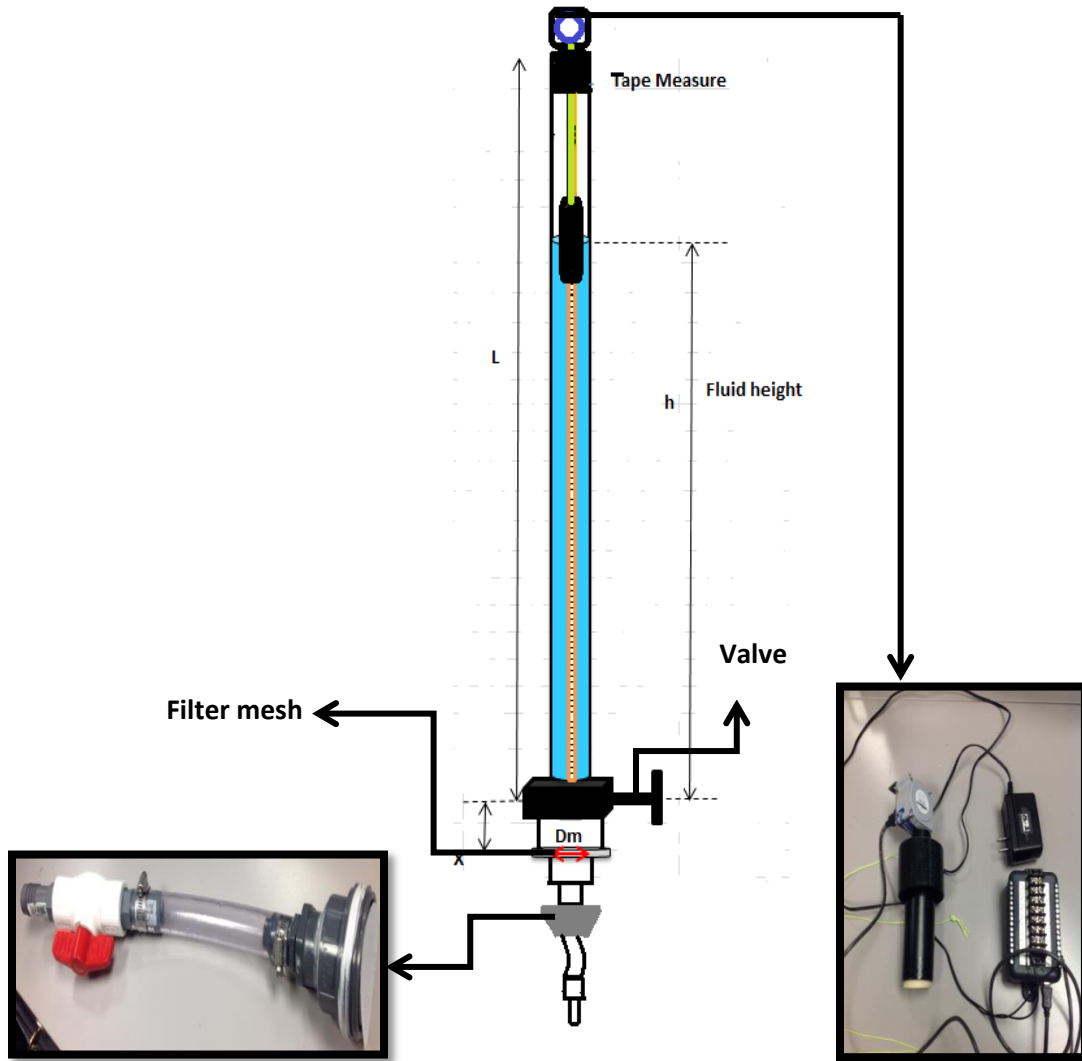


Fig 3.1: Schematic diagram of the bench scale filtration unit.

3.1.3 Calibrating the String Potentiometer:

The calibration of the string potentiometer was accomplished by measuring different heights with the corresponding voltages; they shared a linear relationship (Figure 3.2) i.e. with the increase in height, the voltage increased and vice versa. With the help of the string potentiometer, the steady drainage of the wastewater was recorded and the filtered water was

further processed for analysis of several water quality parameters such as TSS, COD, turbidity and absorbance.

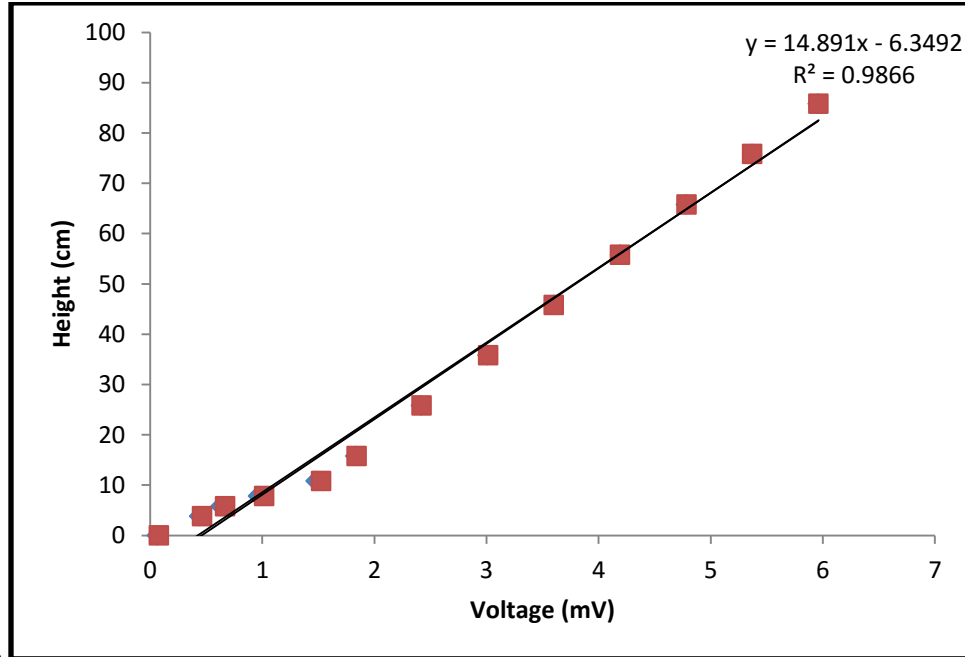


Fig 3.2: Calibration of the string potentiometer.

3.1.4 Development of SOP for the column filtration test:

The filtration column was filled with wastewater (primary influent) collected from the Pottersburg Pollution Control plant located in London, Ontario and the valve was completely opened for the water to flow. The filtered water was then collected continuously in 5 different sample bottles making sure to avoid spilling as much as possible. As the water flowed down the column, the string potentiometer sent signals to the computer, which recorded the water height at that time. The volume of water in the sample bottles was measured and noted. After completing one run, the filter mesh was taken out of the filter column, washed and put back for the next run. It is to be noted here that the column tests were repeated with different mesh sizes, namely 350

µm, and 158 µm. These meshes were made of nylon and manufactured by Salsnes, company which makes the filtration units for treating municipal wastewater.

3.2 Analytical methods:

The samples brought back to the lab were analyzed for TSS, turbidity, absorbance, and COD.

For measurement of TSS, the initial weight of the filter (a 1.2 µm glass fiber filter, VWR Canada) was first noted and then 100 ml of the sample was passed through it. The filter was dried in the oven for 4 hours and the final weight of the filter was measured.

$$\text{TSS} = \frac{\text{Final weight of the filter (g)} - \text{Initial weight of the filter (g)}}{\text{Sample volume (100ml)}} * 10^6$$

For measurement of turbidity, 5 ml of the sample was well shaken and put inside a vial for measuring turbidity using a 2100 HACH turbidimeter. The average of 2 readings was taken for each sample.

The absorbance of the sample was measured at four wavelengths (250 nm, 300 nm, 400 nm and 600 nm), where 200-300 nm range represents the colloidal particles in the wastewater, 400 nm is for yellow color [Georgiou *et al.*,] and 600 nm represents for de-colorization. A Shimadzu spectrophotometer was used to measure UV-VIS absorbance and triplicate readings of each sample were noted and the average absorbance of all three values was determined. The final value of the absorbance was determined by taking an average of all the three values.

The COD of the water samples was measured using the high range HACH COD vials. 2 ml of the sample was poured inside the vial and digested for 2 hours. After 2 hours, the vial was cooled and the total COD in the sample was read using a HACH meter.

Flux was calculated by first calculating the flowrate (Q), subtracting the filtered volume from the initial water level divided by the area (A) of the filter mesh. This was then divided by the height (h) as obtained from the calibrated string potentiometer. Darcy's law at constant pressure difference has been used to calculate flux. It is worth mentioning here that the clean filter flux was calculated using Computational Fluid Dynamics (CFD).

The removal efficiency was calculated by subtracting the influent TSS with the effluent TSS and then divided by the effluent TSS.

3.3 Statistical Software:

Statistical Analysis Software (SAS) version 9.4 was used for model selection and ANOVA (Analysis of Variance) analysis. The SAS program uses AIC (Akaike Information Criterion), BIC (Bayesian Information Criterion) and C_p as its measures of the relative quality of the best fit model. These criteria take into account not only how good the data fit an equation but also account for the complexity of the model giving the lowest score to the optimal model which accounts for both the best fit as well as low score index. After model selection, the variables obtained from the selected model were analyzed using ANOVA which yields the p value, a measure of whether the parameter under consideration (in this case flux) is related to a specific variable keeping all other variables in the model constant. If the p value is less than 0.05 then that particular variable is statistically significant, i.e., if that particular variable is taken out of the

model, flux will change significantly. A subset of variables was created using the lowest score index and highest R-square values. These variables were then further used for future analysis.

JMP version 10 was used as alternative statistical analysis software. JMP has been considered as the “statistical discovery of SAS”. Similar parameters as obtained from SAS were derived using JMP. JMP is user friendly and employs a click and use interface and does not require coding like SAS. It also links powerful dynamic visualization to statistics.

3.4 Regression Software:

The software used for this purpose were HeuristicLab Optimizer 3.3.11.12010 (H.L) and Eureqa 1.10.0 Beta. H.L was created by the HEAL laboratory of University of Upper Austria. The software serves as a framework for heuristic and evolutionary algorithms. Genetic programming (GP) has been used to form the symbolic regression model. The main idea behind symbolic regression as mentioned earlier is to develop a mathematical model that fits the input and output data to satisfy the complex problem. GP has a lot of advantages including no requirement of a priori assumption, capability of distinguishing between relevant and irrelevant inputs, and yielding models, which can represent the system characteristics [McKay *et al.*, 1996]. GP has been used in fields like process control [McKay *et al.*, 1996] [Bettenhausen, 1995] [Marenbach, 1997] [McKay *et al.*, 1997] [Willis *et al.*, 1997] [Hong, 2001], and environmental modeling [Babovic, 1997] [Keijzer, 1999] [Whigham, 1995] [Hong, 1999].

Eureqa was founded by Michael Schimdt in 2011. This software instead of using neural networks and regression trees brings forth the idea of machine learning to de-mystify the relationships between different variables.

The next chapter of this thesis describes the results using the software and the analytical methods described in this chapter.

Chapter 4

Results and Discussions

4.1 Variation in wastewater quality:

The wastewater in a particular region is synonymous with the lifestyles of the people living there. In London, the Pottersburg Pollution Control Plant receives most of its influent wastewater from the industries due to its location. Fig. 4.1 shows the variation in the wastewater sampled over the period of June 2014 – May 2015. The TSS has been averaged over multiple samples collected on the same day. The period of collection included months of snowfall, days of heavy rainfalls, thunderstorms and sunny days.

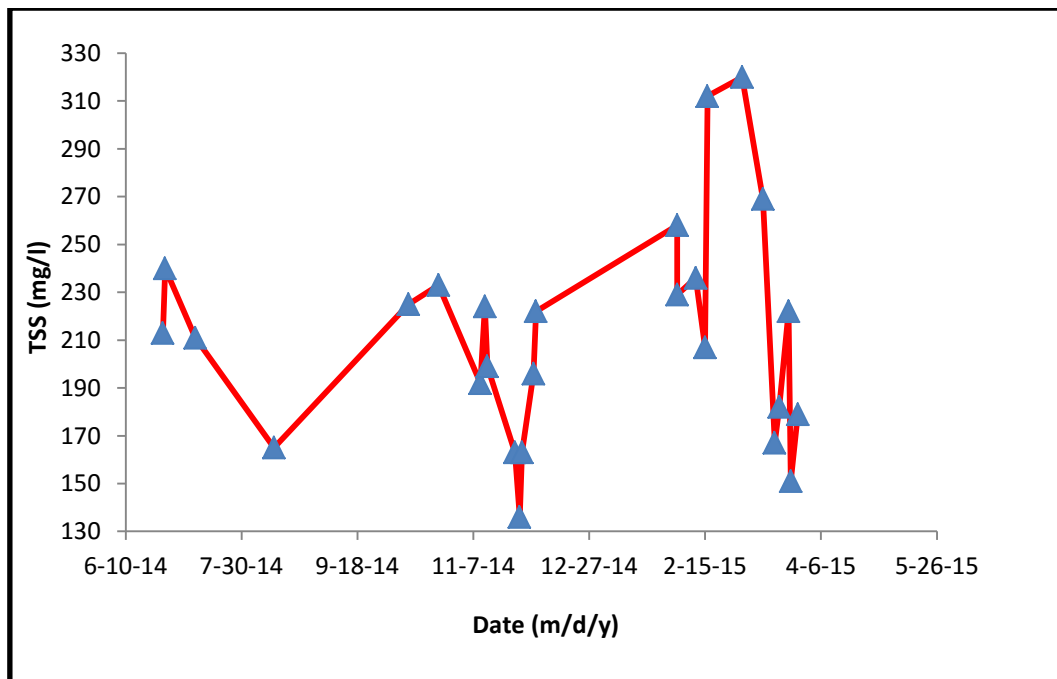


Fig. 4.1: Variations in Wastewater at the Pottersburg Pollution Control Plant.

This winter season (2014) experienced heavy snowfall which led to accumulation of snow on the surfaces. As spring approached, a peak in the month of March – April was observed due to early spring thaw.

During the months of May and June 2015, the experiments were focused mostly at the Adelaide pollution control plant and Greenway pollution control plant. Fig. 4.2 represents the changes in the water quality at the three peak intervals; namely 9.30 AM, 12.30 PM, 3.30 PM taken over a period of May 2015 – June 2015.

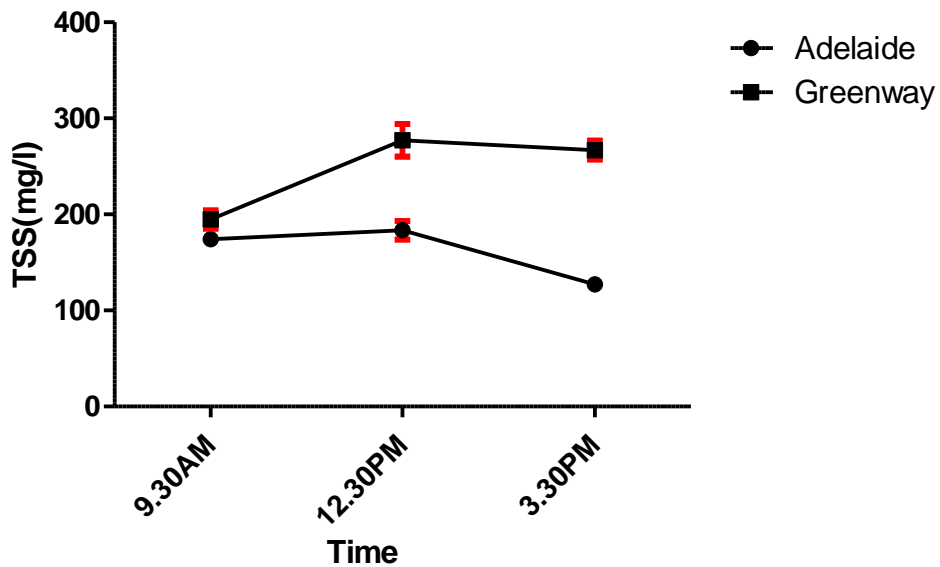


Fig 4.2: Changes in water quality at the Adelaide and Greenway Plants.

The location of the wastewater plants plays a very important role in determining the quality of the wastewater influent entering the plant. The Greenway plant located in west London, receives mostly residential waste. As a result of which the water quality has higher amount of particulate matter than that of either Adelaide or Pottersburg treatment plants. Moreover the primary effluent is often used to flush the sludge lines of the plant and the flush water is then treated

along with the primary influent. Adelaide plant on the other hand has few industries and some residential areas which discharge their effluent into it. At 9.30 AM interval the water quality for both the plants seem to have similar range of particulate solids, but as the time increases, the difference in particulate solids concentration becomes greater. Especially, during the 3.30 PM interval a significant difference can be observed in water qualities collected from the two plants. This could be due to the afternoon activities in residences like showering, cleaning etc. resulting in higher increase of suspended solids.

These variations observed were noted down and they formed an integral part of the modelling approach taken at the very end of data collection.

4.2 Characterizing the filter mesh:

Before obtaining data from the lab scale filtration unit, it was very essential to first characterize the filter mesh. Salsnes had provided the couple of meshes used in this work stating their nominal pore sizes as 350 μm and 158 μm , respectively. A Zeiss microscope with magnification of 100 x was used to determine the actual pore size. Figs. 4.3 and 4.4 represent the pore size of the nylon meshes.

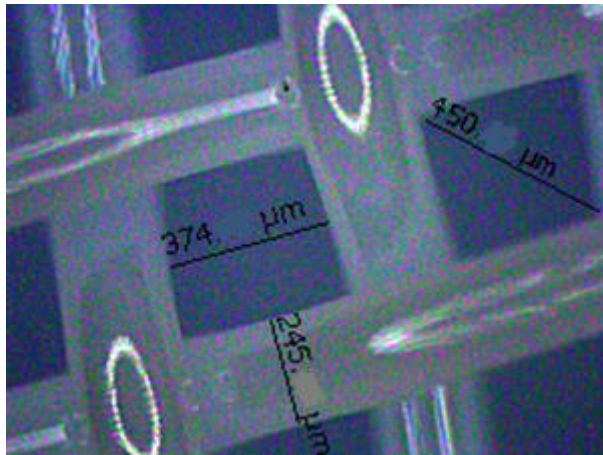


Fig. 4.3: Microscopic measurement of the 350 μm mesh.

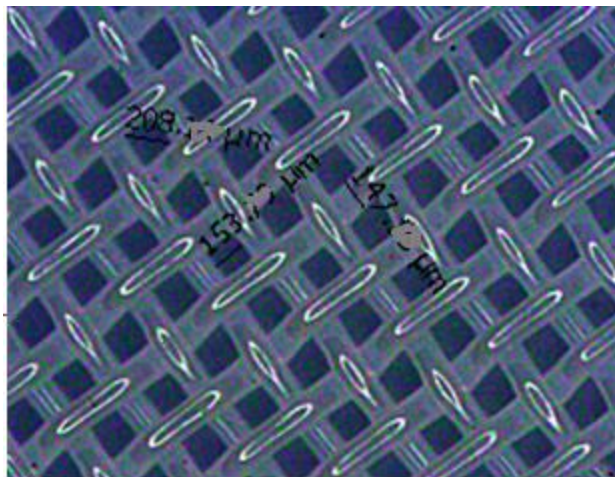


Fig. 4.4: Microscopic measurement of the 158 μm mesh.

Analysis of the images obtained from the microscope shows that the pore size measured horizontally rather than the diagonal distance is closer to the size as stated by Salsnes. The measurements are 374 μm for the 350 μm mesh and 153 μm for the 158 μm mesh.

4.3 First phase of data collection:

On having characterized the filter mesh, the next step was to collect data and embark on building up a database. For this the Pottersburg pollution control wastewater plant was chosen for

collecting water samples due to its location and easy transfer of samples to Trojan Technologies for further processing. This plant located on Gore road; London, Ontario employs all the necessary steps including screens and settling tanks for solids removal, activated sludge to degrade the organic compounds, and finally UV disinfection as the final step.

4.3.1 Building up the database:

A number of parameters were taken into consideration while conducting the experiments at Pottersburg. A total of 75 sets of data were collected in the months from February - March 2015. The complete dataset is presented in the appendix.

The bench scale unit shown in Chapter 3 or the column setup was always filled with 2 liters of primary influent (PI) and the valve was opened for continuous flow of the filtered water. As the water filtered out, it was collected in the sample bottles and the continuous drainage of the water was recorded using a string potentiometer. The samples were brought back to Trojan technologies for post processing and were tested for measurement of TSS, COD, turbidity and absorbance at 250 nm, 300 nm, 400 nm, and 600 nm. The 250 nm – 300 nm is the wavelength for measuring the colloids in the sample. The exact wavelength is 254 nm [Amarasiriwardena. 2001] for measuring the colloidal matter in wastewater. 400 nm and 600nm as mentioned before is for the color yellow and decolorization of wastewater respectively.

As the water drained out of the column, the flux of the filter mesh (350 μm and 158 μm) decreased over time [flux was calculated using Darcy's law] and the particles removal efficiency increased. This is quite expected in dead-end filtration, as the water flows gradually through the filter mesh, a cake like structure is formed which provides further resistance to filtration. This buildup of mass on the filter mesh can be classified into two different categories: concentration

polarization (CP), and formation of a “cake” between the CP layer and the membrane surface. There have been models which have discussed the influence of concentration polarization on permeate flux decline (Kedem and Katchalsky. 1958; Vilker *et al.*, 1981; Reihanian *et al.*, 1983; Bhattacharjee *et al.*, 1994, 1999; Elimelech and Bhattacharjee. 1998). However, in many practical applications, the effect of concentration polarization on permeate flux is rarely measurable as the transition from CP to cake formation occurs almost immediately (Song and Elimelech. 1995). The cake mat as formed is an accumulation of solids present in the wastewater. Figs. 4.5 and 4.6 show how the flux drops as the filter accumulates solids from the water stream. This accumulation of solids on the filter mesh has been termed as Total Suspended Solids accumulated or TSSa.

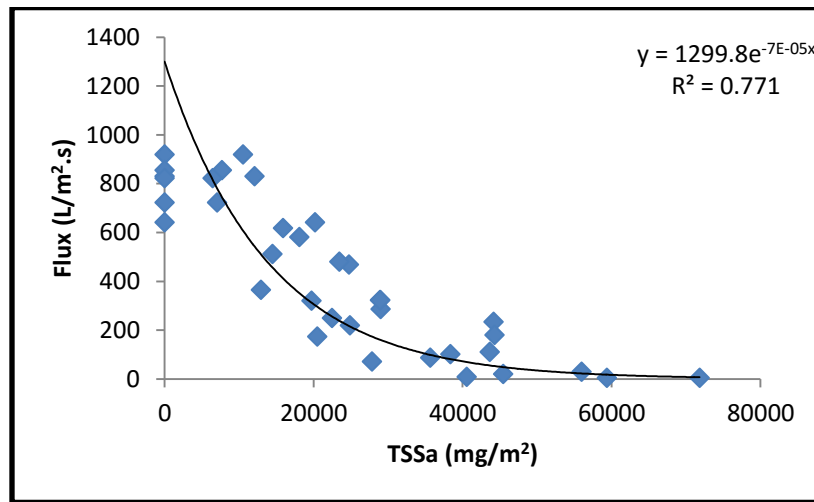


Fig 4.5: Flux vs. TSSa for the 350 µm mesh.

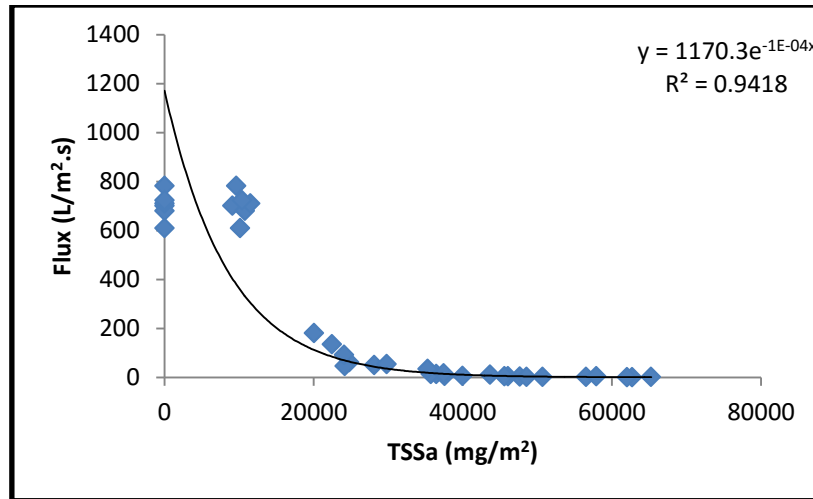


Fig 4.6: Flux vs. TSSa for the 158 µm mesh.

The flux of the 158 µm is lower than the 350 µm as the larger the pore size lower the resistance to the filter and higher the flux. Since at higher amount of TSSa, due to cake filtration the filter mesh would get clogged, hence for 158 µm it was very difficult to drain enough water out for post processing. As the water quality changed, higher the amount of suspended particles and lower the size of the filter mesh, more particles are trapped on the mesh due to increasing resistance offered by the mesh and the cake on it. This results in high TSSa on the mesh with lower flux.

Due to formation of a cake on the filter mesh (Fig. 4.7) a significant reduction of the TSS in the filtrate occurs. The higher the amount of suspended solids in the influent water, thicker the cake formed on the mesh (Fig. 4.8) ultimately resulting in clogging of the mesh. The filter mesh then needs to be taken out, washed and put back in the holder compartment for the next run.



Fig. 4.7: Formation of cake on a filter mesh with TSS of 140 mg/l.



Fig. 4.8: Formation of cake on a filter mesh with TSS of 265 mg/l.

The cake formed on the filter mat, acts as a trap for particles larger than its size and the filtrate continues to be cleaner as the filtration proceeds till it reaches a plateau. The removal efficiency

with regards to the TSS over the filter mesh, versus the total amount of accumulated solids on the filter mesh is shown in Figs. 4.9 and 4.10.

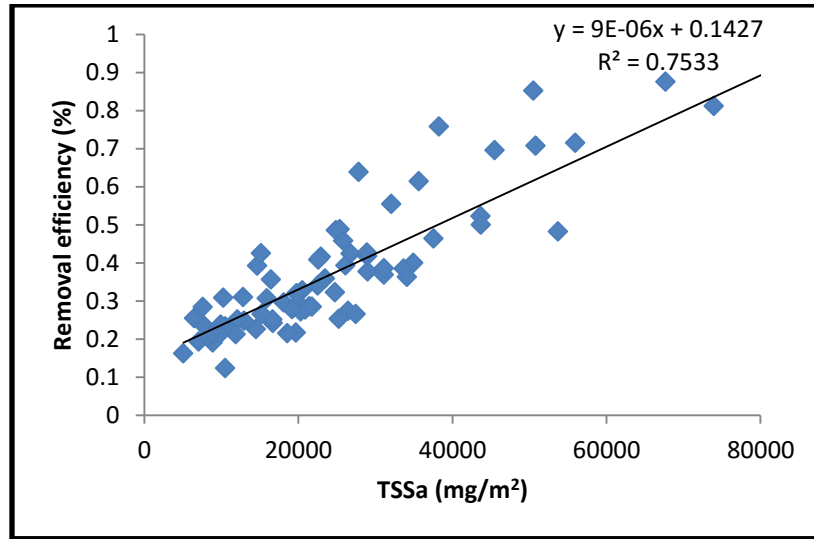


Fig. 4.9: Removal efficiency of the filter mesh vs TSSa for 350 µm

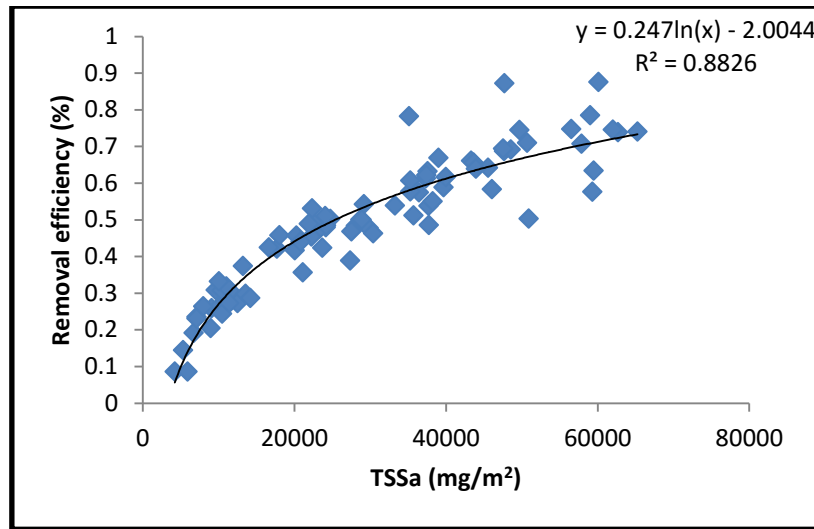


Fig 4.10: Removal efficiency of the filter mesh vs TSSa for 158 µm mesh.

The experiments conducted were always triplicated with the same water quality and were mostly focused at the Pottersburg pollution control plant. This resulted in building up a database with multiple parameters for analyzing the influent water quality.

Co-relations were developed between multiple parameters from the developed database. The first co-relation developed was between COD in the effluent (COD_{eff}) and TSS_{eff} . There occurs a linear relationship between them i.e. with the increase in the TSS_{eff} , COD in the effluent will increase and vice-versa, with a R-squared value of 0.87 (Fig 4.11). The decrease of COD in this case refers to the particulate COD which gets trapped in the filter mesh during the filtration process and thus decreases during filtration. This result is in agreement with the research of Chi (2006) when comparing the slopes where chitosan was used in treating waste stream from the dairy industries.

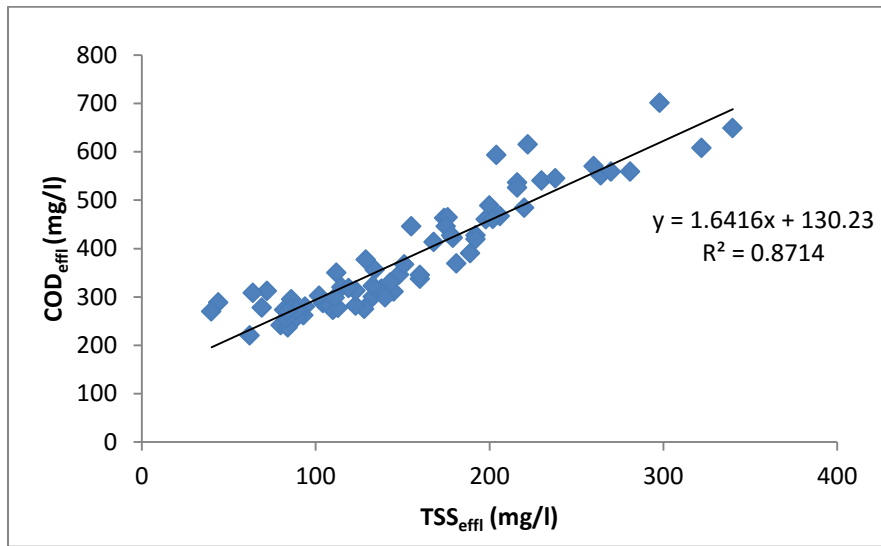


Fig. 4.11: COD_{eff} vs. TSS_{eff} of the filtrate.

The next linear co-relation exists between the turbidity and the TSS with a R-squared of almost 0.90 (Fig. 4.12). Higher the amount of suspended solids in the water, higher is the turbidity. Hannouche *et al.*, (2011) in their research have showed a linear relationship between TSS and turbidity in the effluent while experimenting with combined sewer flow systems.

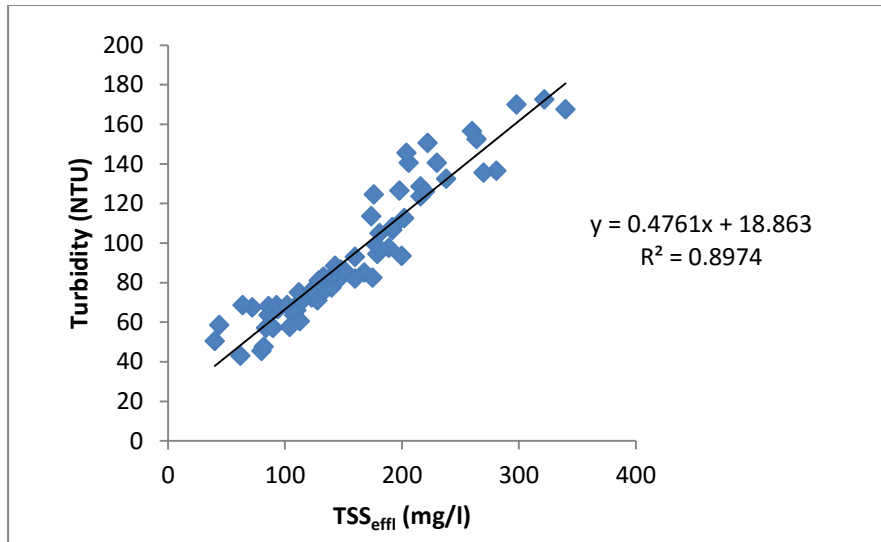


Fig. 4.12: Turbidity vs. TSS_{eff} of the filtrate.

The final co-relation was developed between turbidity and COD with a R-squared of 0.90 (Fig. 4.13). The COD consists of two parts, the particulate COD and soluble COD. So lower the particulate COD, lower would be the turbidity. It is to be noted here that all the turbidity and TSS values correspond to that of the filtrate. Fogelman *et al.*, (2006) developed a technique for measuring COD and then correlated with turbidity to obtain a slope similar to that obtained in this work when the turbidity values were within 150 NTU. In this thesis, the maximum turbidity values recorded were close to 180 NTU and hence a good agreement can be reached between both the results.

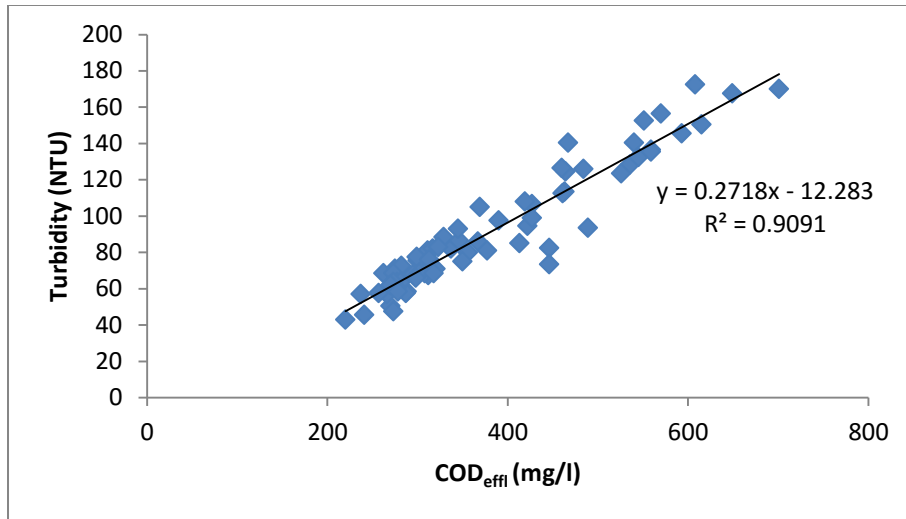


Fig. 4.13: Turbidity vs. COD_{eff} of the filtrate.

4.3.2 Statistical analysis of the database:

After the database was populated with data primarily collected from the Pottersburg pollution control plant, statistical analysis of the data was of utmost importance. For conducting the statistical analysis, two software were used namely: Statistical Analysis Software (SAS) and JMP. SAS uses its own programming language known as “SAS programming language”. As this thesis aims to find the right water quality parameters to correlate and model flux, the code was written to first predict a model with flux as a function of the rest of the parameters and then its statistical significance (refer to appendix). All the 3 criteria namely AIC, BIC and Cp predicted the model of flux as a function of multiple water quality parameters (Tables 4.1, 4.2 and 4.3).

Table 4.1: Best 10 models predicted by the AIC algorithm

Best 10 models by AIC										
Obs	Model	Dependent	ModelIndex	NumInModel	Cp	RSquare	Control	AIC	SBC	VarsInModel
1	MODEL1	Permeability	1	7	5.2652	0.8199		725.7152	743.92856	TSSa TSSin I2c Turbidity350 TCOD350 TCOD158 TSSSVout
2	MODEL1	Permeability	20	9	7.0259	0.8265		727.0343	749.80094	TSSa Mesh TSSin I3c I4c Turbidity350 TCOD350 TCOD158 TSSSVout
3	MODEL1	Permeability	17	8	6.7222	0.8215		727.0743	747.56428	TSSa TSSin I2c I3c Turbidity350 TCOD350 TCOD158 TSSSVout
4	MODEL1	Permeability	21	9	7.1183	0.8262		727.1469	749.91351	TSSa Mesh TSSin I1c I3c I4c Turbidity350 TCOD350 TCOD158
5	MODEL1	Permeability	37	9	7.2103	0.8259		727.2588	750.02550	TSSa Mesh TSSin I1c I3c I4c Turbidity158 TCOD350 TCOD158
6	MODEL1	Permeability	19	8	6.9054	0.8209		727.2911	747.78109	TSSa TSSin I2c Turbidity350 Turbidity158 TCOD350 TCOD158 TSSSVout
7	MODEL1	Permeability	54	9	7.3512	0.8255		727.4300	750.19667	TSSa TSSin I2c I3c Turbidity350 Turbidity158 TCOD350 TCOD158 TSSSVout
8	MODEL1	Permeability	18	7	6.8147	0.8153		727.5136	745.72696	TSSa Mesh TSSin I4c Turbidity158 TCOD350 TCOD158
9	MODEL1	Permeability	22	8	7.1350	0.8203		727.5620	748.05200	TSSa Mesh TSSin I2c Turbidity350 TCOD350 TCOD158 TSSSVout
10	MODEL1	Permeability	38	8	7.2213	0.8200		727.6636	748.15359	TSSa TSSin I1c I2c Turbidity350 TCOD350 TCOD158 TSSSVout

Table 4.2: Best 10 models predicted by the BIC algorithm

Best 10 models by BIC										
Obs	Model	Dependent	ModelIndex	NumInModel	Cp	RSquare	Control	AIC	SBC	VarsInModel
1	MODEL1	Permeability	2	4	6.5207	0.7986		727.7737	739.15703	TSSa Mesh TSSin Turbidity350
2	MODEL1	Permeability	3	4	6.6986	0.7980		727.9605	739.34379	TSSa TSSin TSSSVout SvEff158
3	MODEL1	Permeability	4	4	6.6986	0.7980		727.9605	739.34379	TSSa TSSin SV1158 TSSSVout
4	MODEL1	Permeability	5	4	6.6986	0.7980		727.9605	739.34379	TSSa TSSin SV3350 TSSSVout
5	MODEL1	Permeability	6	4	6.6986	0.7980		727.9605	739.34379	TSSa TSSin SV3158 TSSSVout
6	MODEL1	Permeability	7	4	6.6986	0.7980		727.9605	739.34379	TSSa TSSin SVturb350 TSSSVout
7	MODEL1	Permeability	8	4	6.6986	0.7980		727.9605	739.34379	TSSa TSSin SVTCOD350 TSSSVout
8	MODEL1	Permeability	9	4	6.6986	0.7980		727.9605	739.34379	TSSa TSSin SVturb158 TSSSVout
9	MODEL1	Permeability	10	4	6.6986	0.7980		727.9605	739.34379	TSSa TSSin SVTCOD158 TSSSVout
10	MODEL1	Permeability	11	4	6.6986	0.7980		727.9605	739.34379	TSSa TSSin SV2158 TSSSVout

Table 4.3: Best 10 models predicted by the Cp algorithm.

Number in Model	C(p)	R-Square	AIC	SBC	Variables in Model
7	5.2652	0.8199	725.7152	743.92856	TSSa TSSin I2c Turbidity350 TCOD350 TCOD158 TSSSVout
4	6.5207	0.7986	727.7737	739.15703	TSSa Mesh TSSin Turbidity350
4	6.6986	0.7980	727.9605	739.34379	TSSa TSSin TSSSVout SvEff158
4	6.6986	0.7980	727.9605	739.34379	TSSa TSSin SM1158 TSSSVout
4	6.6986	0.7980	727.9605	739.34379	TSSa TSSin SM3350 TSSSVout
4	6.6986	0.7980	727.9605	739.34379	TSSa TSSin SM3158 TSSSVout
4	6.6986	0.7980	727.9605	739.34379	TSSa TSSin SVturb350 TSSSVout
4	6.6986	0.7980	727.9605	739.34379	TSSa TSSin SVTCOD350 TSSSVout
4	6.6986	0.7980	727.9605	739.34379	TSSa TSSin SVturb158 TSSSVout
4	6.6986	0.7980	727.9605	739.34379	TSSa TSSin SVTCOD158 TSSSVout

The criterion for model selection is the one with the lowest score index. As a result of which a subset of all the variables was created with the highest R-squared value and lowest score from each algorithm. The first 10 models were selected as those are the most important ones. On conducting an ANOVA analysis with the selected parameters with a 95% confidence level, the predicted parameters having a p value less than 0.05 were TSSa, mesh, absorbance at wavelength 400 nm, absorbance at wavelength 600 nm, turbidity, COD, influent TSS, sieved sample TSS (Table 4.4).

Table 4.4: Statistical analysis using SAS

Source	DF	Sum of Squares	Mean Square	F Value	Pr > F
Model	9	6308448.712	700938.746	32.81	<.0001
Error	62	1324554.312	21363.779		
Corrected Total	71	7633003.024			

R-Square	Coeff Var	Root MSE	Permeability Mean
0.826470	42.97849	146.1635	340.0853

Source	DF	Type III SS	Mean Square	F Value	Pr > F
TSSa	1	5401686.388	5401686.388	252.84	<.0001
Mesh	1	97596.885	97596.885	4.57	0.0365
TSSin	1	327372.249	327372.249	15.32	0.0002
l3c	1	126295.075	126295.075	5.91	0.0179
l4c	1	117492.598	117492.598	5.50	0.0222
Turbidity350	1	67102.127	67102.127	3.14	0.0813
TCOD350	1	203663.380	203663.380	9.53	0.0030
TCOD158	1	129900.902	129900.902	6.08	0.0164
TSSSVout	1	71627.276	71627.276	3.35	0.0719

Parameter	Estimate	Standard Error	t Value	Pr > t
Intercept	1443.68098	422.159452	3.42	0.0011
TSSa	-0.01508	0.000948	-15.90	<.0001
Mesh	0.70316	0.328984	2.14	0.0365
TSSin	15.22120	3.888364	3.91	0.0002
l3c	-6032.44840	2481.072460	-2.43	0.0179
l4c	-14388.77477	6135.607948	-2.35	0.0222
Turbidity350	-10.84328	6.118309	-1.77	0.0813
TCOD350	-6.61083	2.141109	-3.09	0.0030
TCOD158	1.31983	0.535243	2.47	0.0164
TSSSVout	7.07214	3.862343	1.83	0.0719

Similar statistical analysis was conducted with JMP, which in turn yielded the same results (Table 4.5) like SAS. The only difference between both the software is that JMP is more visually and graphically insightful than SAS. A plot of the predicted and actual flux has been shown below (Fig. 4.14)

Table 4.5: JMP analysis

Summary of Fit				
RSquare		0.821631		
RSquare Adj		0.795739		
Root Mean Square Error		148.1876		
Mean of Response		340.0853		
Observations (or Sum Wgts)		72		

Analysis of Variance				
Source	DF	Sum of Squares	Mean Square	F Ratio
Model	9	6271510.8	696835	31.7326
Error	62	1361492.2	21960	Prob > F
C. Total	71	7633003.0		<.0001*

Parameter Estimates				
Term	Estimate	Std Error	t Ratio	Prob> t
Intercept	1594.5161	418.8395	3.81	0.0003*
TSSa	-0.01531	0.000991	-15.45	<.0001*
Mesh	1.3185304	0.318218	4.14	0.0001*
TSSin	17.278949	5.103812	3.39	0.0012*
I3c	-5630.945	2784.545	-2.02	0.0475*
I4c	-19375.63	7819.244	-2.48	0.0160*
SVI1350	2204.9464	1754.331	1.26	0.2135
Turbidity350	-15.4195	7.230208	-2.13	0.0369*
TCOD350	-8.014835	3.306743	-2.42	0.0183*
TCOD158	1.7426123	0.693835	2.51	0.0146*

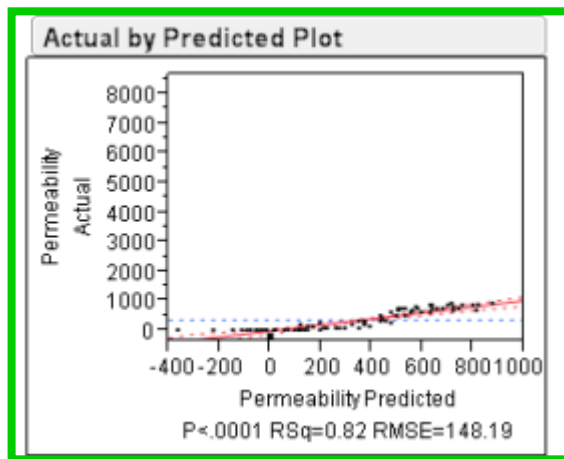


Fig. 4.14: Actual vs. predicted flux as predicted by JMP.

All these models were linear in nature, therefore, the next step was to search for a non-linear relationship between them if there was any improvement in the model accuracy. For this, symbolic regression was used using Eureqa and HeuristicLab (H.L) software.

H.L uses genetic programming to assess such relationships between different variables. 66% of the datasets collected over time in populating the database were used to first train the model and the rest 34% was used for validation purposes. Statistically significant parameters as evaluated before were fed to the program to not only find a non-linear relationship, but also reduce the number of parameters. A funneling approach was used to eliminate as many parameters while obtaining the best possible results. Out of all the 8 parameters, H.L further shortened the list to a total of 4 parameters namely TSSa, TSS_{in}, mesh and turbidity (Figure 4.15).

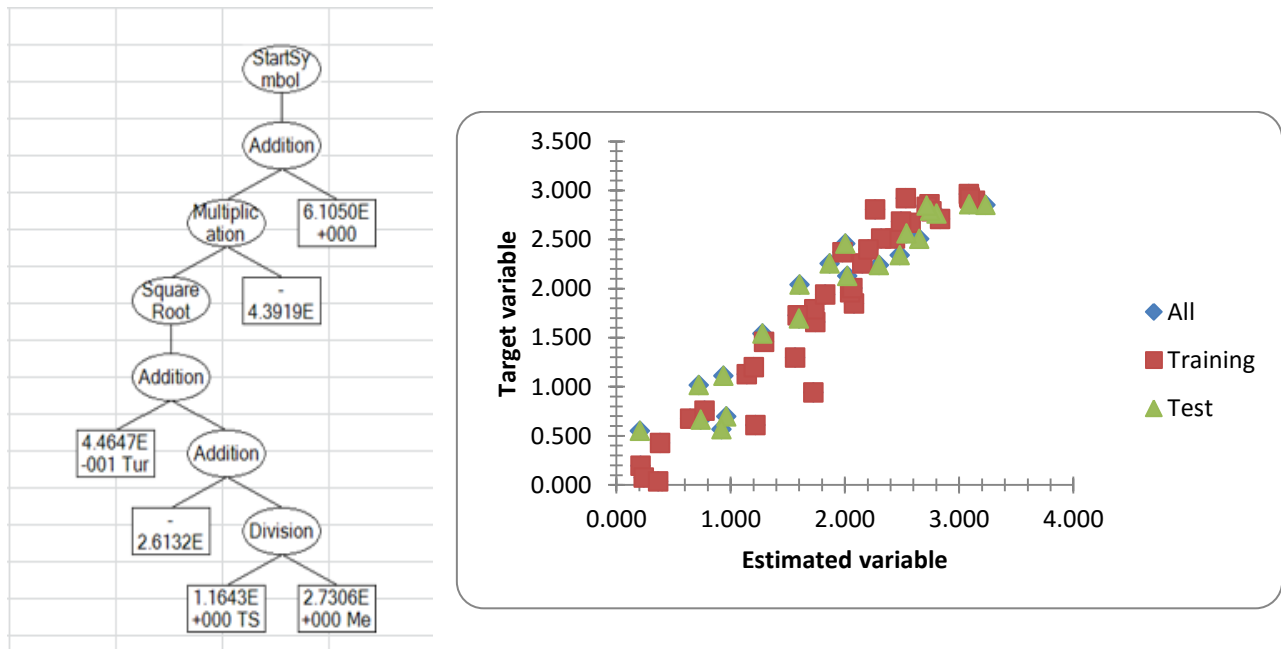


Fig.4.15 : Analysis using HeuristicLab

The regression tree (Fig. 4.15) gives an indication of the most important parameters necessary to predict flux and also helps in constructing the non-linear equation for the model. The scatter plot shows how the observed values match with the predicted values and the line chart shows how well the H.L can train itself with the target values.

Eureqa, instead of using neural networks and regression trees brings forth the idea of machine learning to de-mystify the relationships between different variables. The same approach was applied as that in H.L; 66% of the database was used for training the software and 34% was used for validation. Eureqa predicted the same 4 parameters responsible for predicting flux; TSS_a, TSS_{in}, mesh and turbidity (refer to appendix).

Regression analysis helped in finding the best three parameters for predicting flux. With these parameters in mind, experiments were designed taking into consideration all the wastewater plants in London, but due to limited time only samples from Greenway and Adelaide pollution control plants were analyzed.

4.4 Second phase of data collection:

The second phase of data collection was targeted at the Adelaide and Greenway pollution control plants. Three very specific time intervals were chosen considering the peak flow namely 9:30AM, 12:30PM and 3:30PM. Every time interval was duplicated for each plant and 5 repeats of each mesh were conducted. For the complete dataset, please refer to appendix.

During days of heavy rainfall, and thunderstorm, water coming into the plant is dilute due to large volume of water associated with rain, and there is a significant variation in the particle size of the pollutants. As a result, water will spill out during the filtration experiments causing failure

of the experiment. To avoid this, a datasheet was programmed in excel to account for equal distribution of the spilled water.

4.4.1 Modified datasheet:

The modified datasheet (Table 4.6) was created to sort out the anomalies in data obtained during experimentation. The left side of Table 4.6 represents the actual data and has been labeled as “Raw Data”. The column labeled “Controls” hold the key in this datasheet. Under Controls, the column labeled “Combine with next point”, takes either the numerical values of 1 for yes and 0 for no. When these numerical values (1 or 0) are entered for each data point, it either results in combination of the values present in the very next cell or no combination, respectively. When the results are combined, it shifts the formulated value one block upwards. It is worth mentioning here that each parameter (for e.g., filtrate volume, TSS) the formulas are different and combining each value is dependent on the individual formula. The flowsheet for programming has been given below (Fig. 4.16).

Table 4.6: Modified Datasheet.

Constants																						
Condition Area	0.0020268																					
Raw Data					Controls					Calculations												
Case ID	Elapsed Time [s]	Filtrate Volume [L]	TSS out [mg/L]	TSS in [mg/L]	Initial Water Level [m]	Combine With Next Point? 1=Yes 0=No	Point ID Without Combining	Point ID With Combining	Modified Time [s]	Modified Filtrate Volume [L]	Use This Row?	Modified TSS [mg/L]	Water Level [m]	Actual Height used	Mass Removed [mg]	Cumulative Mass Removed [mg]	Effective Mass Removed Per Unit Area [mg/m ²]	Average Time [s]	Average Q/A [m/s]	Average H [m]	Average K [L/s/m ³]	Removal Efficiency [%]
1	0	0	162	162	0.99	0	0	0	0	0	TRUE	162	0.99		0	0	0					
1	0.675	0.79	138	162	0.99	1	1	1	1.425	1.21	TRUE	137	0.393	1055.880952	30.3	30.3	14949.67	0.7125	418.34751	0.6915	605.9533	15.5%
1	1.425	0.42	135	162	0.99	0	2	1	2.35	0.25	TRUE	121	0.26965	684.8626254	10.25	40.55	20006.91	1.8875	133.34827	0.3313	402.4682	25.3%
1	2.35	0.25	121	162	0.99	0	3	2	3	0.11	TRUE	105	0.21538	242.9526241	6.27	46.82	23100.45	2.675	83.496531	0.2425	344.2325	35.2%
1	3	0.11	105	162	0.99	0	4	3	3.85	0.11	TRUE	53	0.16111	446.6672768	11.99	58.81	29016.18	3.425	63.850288	0.1882	339.1898	67.3%
1	3.85	0.11	53	162	0.99	0	5	4	0	0	FALSE	FALSE	FALSE	FALSE	FALSE	FALSE	FALSE	FALSE	FALSE	FALSE	FALSE	FALSE
2	0	0	162	162	1.03	0	0	0	0	0	TRUE	162	1.03		0	0	0					
2	0.45	0.57	139	162	1.03	0	1	1	0.45	0.57	TRUE	139	0.74877	708.6316033	13.11	13.11	6468.324	0.225	624.95888	0.8894	702.6871	14.2%
2	1.1	0.54	138	162	1.03	0	2	2	1.1	0.54	TRUE	138	0.48234	676.589066	12.96	26.07	12862.64	0.775	409.83206	0.6156	665.8918	14.8%
2	1.95	0.32	123	162	1.03	0	3	3	1.95	0.32	TRUE	123	0.32445	466.4726513	12.48	38.55	19020.13	1.525	185.74629	0.4034	460.4559	24.1%
2	3.725	0.25	103	162	1.03	0	4	4	3.725	0.25	TRUE	103	0.20111	269.4686263	14.75	53.3	26297.61	2.8375	69.491351	0.2628	264.4461	36.4%
2	4.9	0.11	53	162	1.03	0	5	5	4.9	0.11	TRUE	53	0.14683	267.6871244	11.33	64.63	31687.7	4.3125	46.18957	0.174	265.5019	63.6%

Measured values: Time, Filtered volume,
TSS_{in}, TSS_{effl}, Initial water level.

Combine with next point?
1 = Yes; 0 = No.

Yes → Combines the values of the current cell and the very next cell
and shifts the sum one row up.

No ↓

The values remain unchanged.

Point Id without combining. Point Id with combining.

Used for references. Point id with combining indicates which values
have been combined.

Modified time:
MAX(IF(Point ID without combining = Point Id with combining))

This comparison would occur with all the points in the
"Point id with combining" in a particular set of data.

Yes → Enter actual time

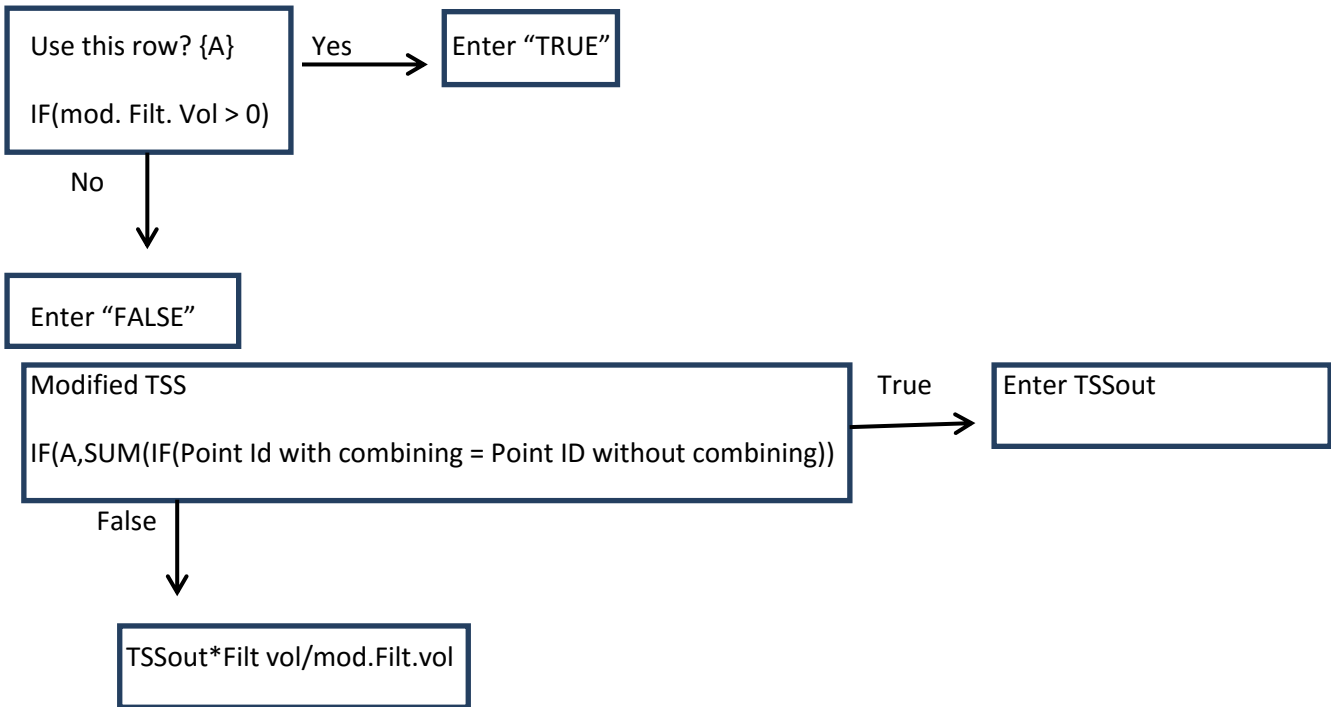
No ↓

Return the max time point

Modified Filtered Volume:
SUM(IF(point ID without combining = Point ID with combining))

Yes → Enter actual filtered volume

No → Return the sum of the filtered volumes



Water level
 $IF(A, \text{Previous water level} - \text{mod. Filt. Vol}/1000/F.\text{Area})$

Mass removed
 $IF(A, (\text{TSS}_{in} - \text{mod. TSS}_{effi}) * \text{mod. Filt vol.})$

Cumulative. Mass removed
 $IF(A, \text{Cumulative mass}/F.\text{Area})$

Average Time (T)
 $IF(A, (T_{n+1} + T_n)/2)$

Average Q/A
 $IF(A, \text{mod. Filt vol}/(T_{n+1} - T_n)/2)$

Average H
 $IF(A, (H_{n+1} + H_n)/2)$

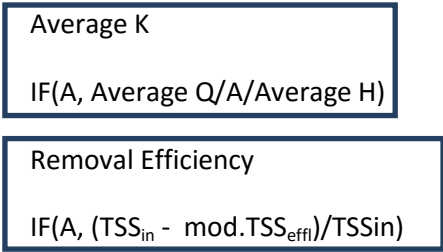


Fig. 4.16: Flowchart for the programming the modified datasheet.

4.5 Regression analysis:

The datasets collected from Adelaide and Greenway pollution control plant were fed to the regression software Eureqa and H.L. The database was a mix of low and high range of TSS values. As obtained from previous regression analysis, turbidity, mesh, TSS_{in} and TSSa are most important for predicting flux; these parameters were only used while building up this database. After sorting the datasets in proper column, the data were used for regression analysis.

For H.L, 100,000 generations were put into place along with the regular mathematical operators (+, -, *, /) and special functions such as logarithm, exponential and power. The length and depth of the regression tree was kept at 10 and 10 respectively to avoid complexity. Upon convergence, the regression tree (Fig. 4.17) yielded the equation relating flux with the other parameters (Eq. 4.1).

$$\textit{Permeability} = \frac{\exp(-0.014 * \textit{TSSa} * 1.653 * \textit{Turbidity})}{((1.038 * \textit{Mesh} + 0.887 * \textit{TSSin}) * 0.015 + 7.003)}$$

..... (4.1)

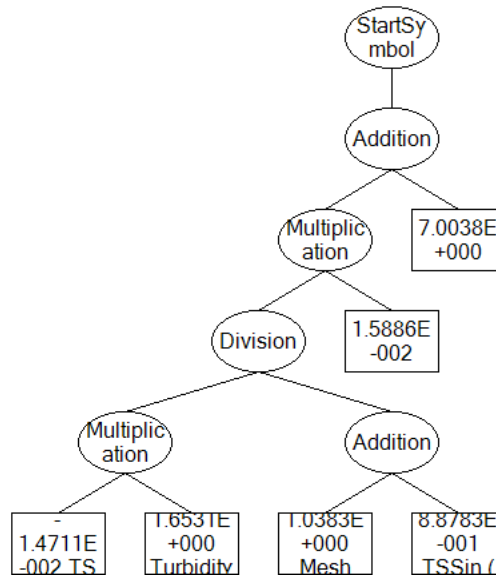


Fig. 4.17: Regression tree obtained from H.L

The equation relates flux as an exponential function of TSSa, turbidity, TSS_{in} and mesh. Before running the regression analysis, all the experimentally calculated values of the flux were converted to log scale to avoid the huge variations and to obtain a more accurate model.

Using Eureqa, the results were similar but the equation was somewhat different (Eq. 4.2). Flux was yet again predicted as an exponential function of mesh, TSSa, TSS_{in}, and turbidity but the constants associated with this equation were different from those of H.L.

Permeability

$$\begin{aligned}
 &= \exp((6.942 + 0.003 * Mesh + 0.009 * TSSin * TSSa \\
 &+ 0.0002 * Mesh * TSSa - 0.258 * TSSa - 3.839 * 10^{-6} \\
 &* TSSa * TSSin * Turbidity - 4.218 * 10^{-6} * Turbidity \\
 &* (TSSa)^2)
 \end{aligned}$$

..... (4.2)

The predicted flux values were separated according to the mesh sizes and plotted against the TSSa on the filter. Fig. 4.18 gives an indication of the decrease in flux as solids accumulated on the filter. The model thus obtained is related well to what was observed experimentally and calculated theoretically using the Darcy's law.

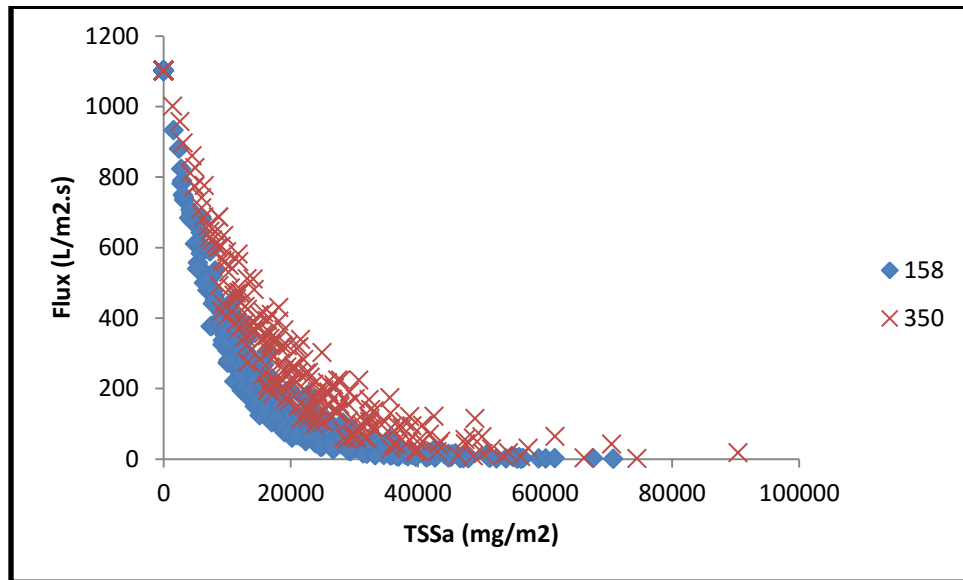


Fig. 4.18: Modelling flux vs. TSSa

4.5.1 Validation of the flux model:

The equations derived must not only be checked for accuracy but also should be validated. While doing so the first step was to find out how close are the predictions between both software were even after having completely different equations from Eureka and H.L. The values obtained from both the equations seem to overlap thus confirming the fact that the predictions by both the software are well matched. A closer look on the predictions for both the equations reveals how

close the predicted values are (Fig. 4.19). Though the prediction algorithms are different for both the software; H.L uses genetic programming while Eureqa uses machine learning to look into different relationships between variables, the predicted values lie on the same line and share a R-Square of value of 0.94.

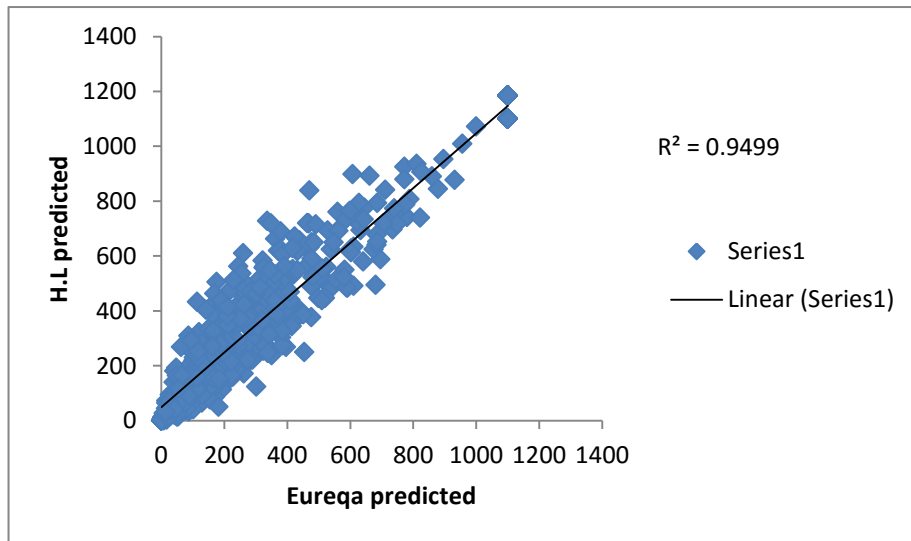


Fig. 4.19: H.L and Eureqa predicted values for flux.

The final step for validating the model for flux was by forming a random database made of turbidity, mesh, TSS_a and TSS_{in}. The values for these parameters were varied keeping one parameter constant at a time and changing the others accordingly (Fig. 4.20). The main aim of doing this was to make sure that at higher values of TSS_a the flux should not drop so much to reach negative values. The cut-off value for TSS_a was 100,000mg/m² of accumulated solids on the filter mesh. Experimental values and theoretical calculations show that the TSS_a reaches a maximum value of 75,000 mg/m² for 1 run before the filter mesh was exhausted and taken out to clean for the next run. Hence 100,000 mg/m² seems to be a reasonable number to validate the model.

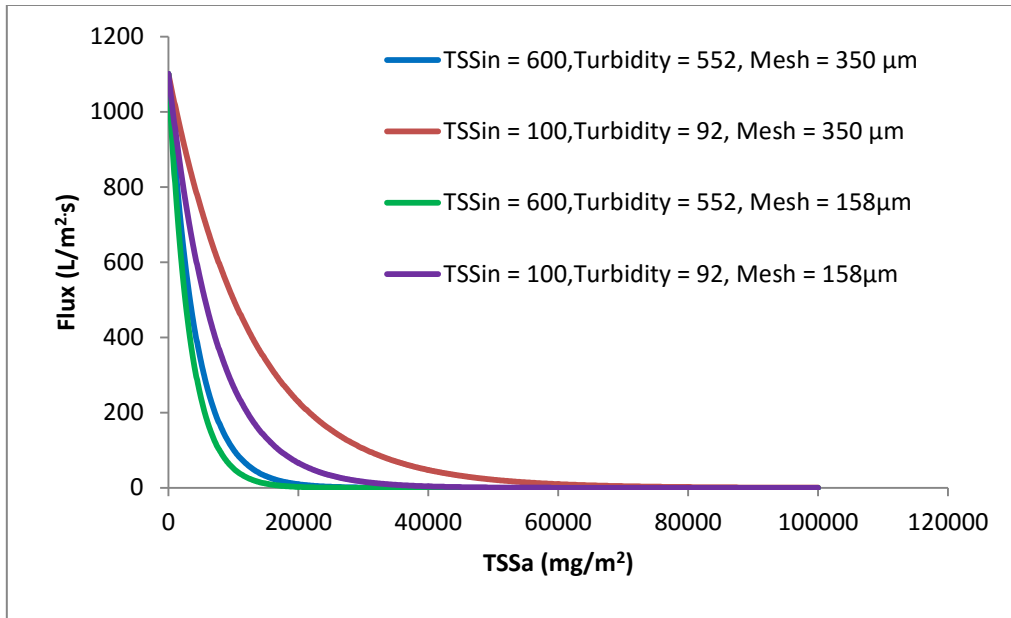


Fig. 4.20: Flux model using random values

Fig. 4.20 describes the decay in flux with solid accumulation on the filter mesh. Higher the amount of TSS in the water sample, the rate at which the flux decreases is faster in a lower mesh size (158 μm) than in higher mesh size (350 μm). Similarly the lower the amount of TSS in the water stream, the drop in flux is faster in 158μm compared to 350μm. This is due to the fact that larger the pore size of the mesh, lower is the resistance and smaller the pore size higher the resistance to the particulates in the water sample. This proves that the particle size in the influent water stream plays a very important role on deciding the flux curves. Every influent wastewater stream entering the wastewater plant is somewhat unique in its own way. The streams generated from industries, households and even from the wastewater plants where the recycled water is used to flush the sludge lines, clean clarifiers and other odd plant jobs, have very different

particle size. This was observed during conducting the experiments and should be made a part of the model in future.

4.5.2 Validation of the removal efficiency model:

The decay in the flux of the filter mesh can also be related to the increase in removal efficiency due to the formation of a cake on the filter. While trying to get the best fit model for removal efficiency, the data were fed for regression similar to the flux modelling, the only difference being the flux being replaced by the removal efficiency. Fig. 4.21 shows the regression tree obtained from H.L.

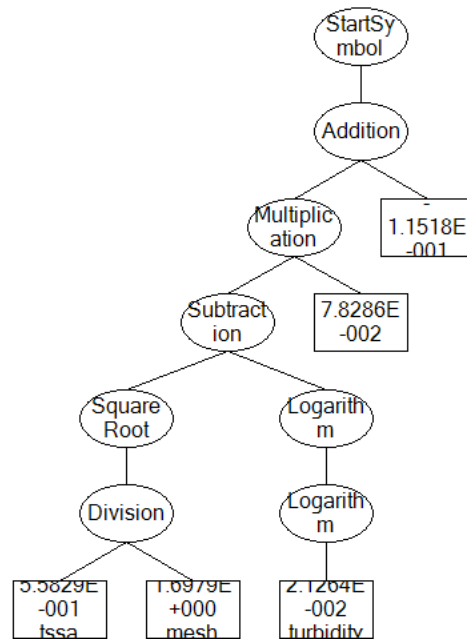


Fig. 4.21: Regression tree obtained from H.L for removal efficiency.

This regression tree from H.L for the model reads as:

Removal efficiency

$$= \left(\left(\text{sqrt} \left(0.558 * \frac{TSSa}{1.697 * Mesh} \right) - LN(LN(0.0212 * Turbidity)) \right) * 0.0782 + -0.115 \right) \dots\dots\dots (4.3)$$

The equation (Eq. 4.3) can predict removal efficiency with TSSa, mesh and turbidity. It does not need TSS_{in} as a parameter to predict the removal efficiency.

Analysis with Eureka revealed a different equation (Eq. 4.4) with other constants. The dependence on certain factors like TSSa, mesh and turbidity was very noticeable.

Removal efficiency

$$= \frac{(2.77 * Turbidity + 0.005 * Turbidity * TSSin)}{(35 * Turbidity + 0.4 * TSSin + Mesh * Turbidity + Turbidity^2 - 9.23 * 10^3)} \dots\dots\dots (4.4)$$

With Eureka, the removal efficiency prediction needed the TSS_{in} unlike that in H.L. With the equations, the next step was to check how close the predicted values for both the software were. Fig. 4.22 shows the observed experimental values of removal efficiencies against the predicted values by both the software's.

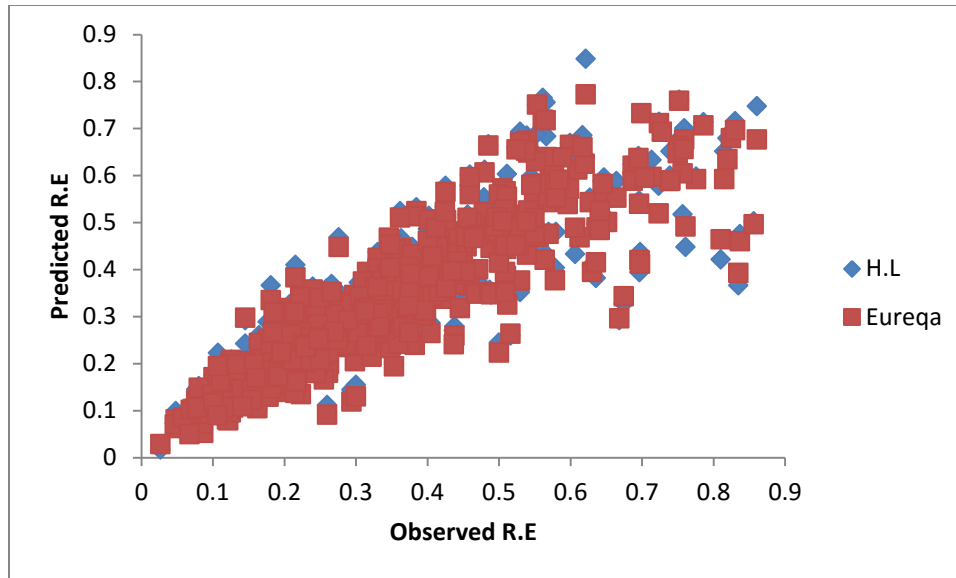


Fig. 4.22: Observed vs. Predicted removal efficiency

The values yet again overlap in most cases showing how closely both the software predicts the values.

The final step in validation of the model was using the same approach as in flux; the use of a random database. While doing so, it was observed that with Eureka (Fig. 4.23) higher the TSS, removal efficiency almost increases in a linear or an exponential manner for both 350 μm and 158 μm meshes. On the other hand, for lower TSS values both the removal efficiencies of the meshes almost reached a plateau where the membrane being clogged resulting in very little increase in removal efficiency.

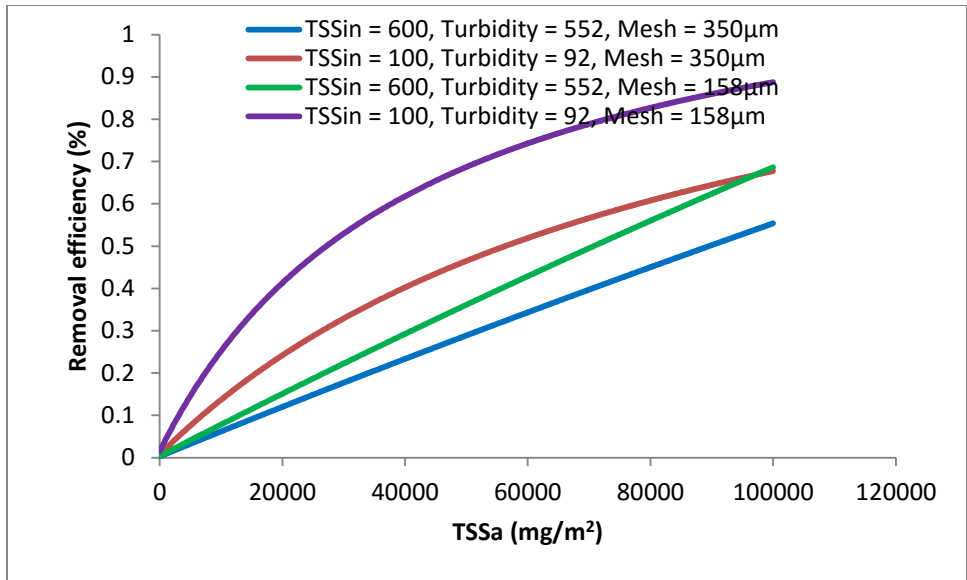


Fig. 4.23: Removal efficiency model predicted by Eureka

The main goal behind this validation process was to determine if at very low TSSa values the removal efficiency would go below zero or become negative. With Eureka, the removal efficiency at TSSa = 0, was 0 but never negative but while doing the same analysis with H.L, this criterion was never satisfied (Fig. 4.24).

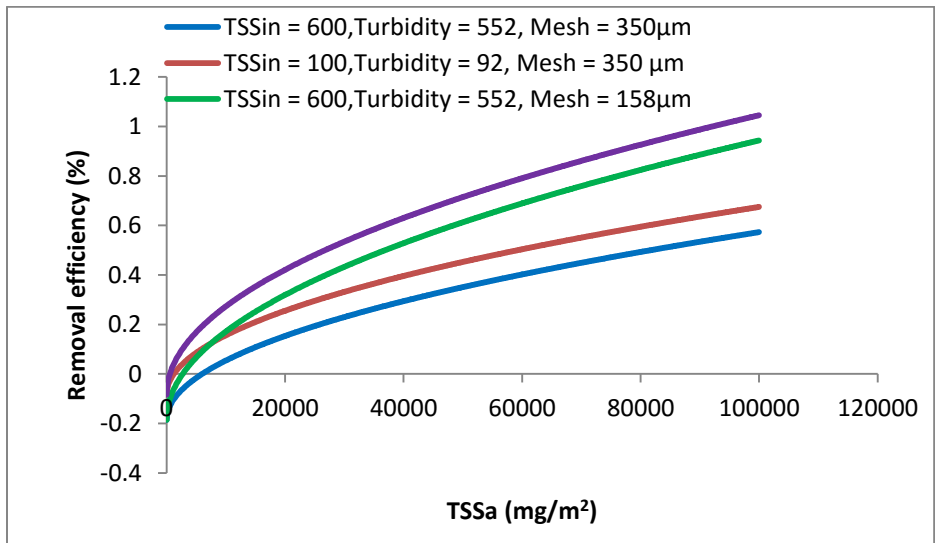


Fig. 4.24: Removal efficiency model predicted by H.L

In Fig. 4.24, clearly the predicted removal efficiencies are below zero or negative at $TSS_a = 0$ which is unrealistic. Moreover the model predicts over 100% removal efficiency which is clearly not valid. The cake formation on the mat would only enhance the cleaner filtrate to pass through (till it gets completely clogged) thus increasing the removal efficiency and not decreasing the efficiency. After careful analysis of the models and keeping all the above discussed factors the model formulated by Eureka best predicts the removal efficiency of a specific dead-end filtration unit.

4.6 Response Surface Models:

The main objective of using a Response Surface Methodology (RSM) is in determining the optimal response by conducting a series of designed experiments thus determining the inter-relationships between the different variables. The dataset used for regression analysis was fed to MiniTab to investigate the surface plot of removal efficiency with the other variables. When doing so, a full factorial design was considered and removal efficiency was plotted against turbidity, mesh, TSS_a , TSS_{in} and a new variable called plant was added. The plant refers to the wastewater plants where the final phase of experiments were conducted namely Greenway and Adelaide pollution control plants. For Greenway plant, a numerical value of 0 was assigned and for Adelaide 1 was assigned. Fig. 4.25 denotes the response surface model obtained.

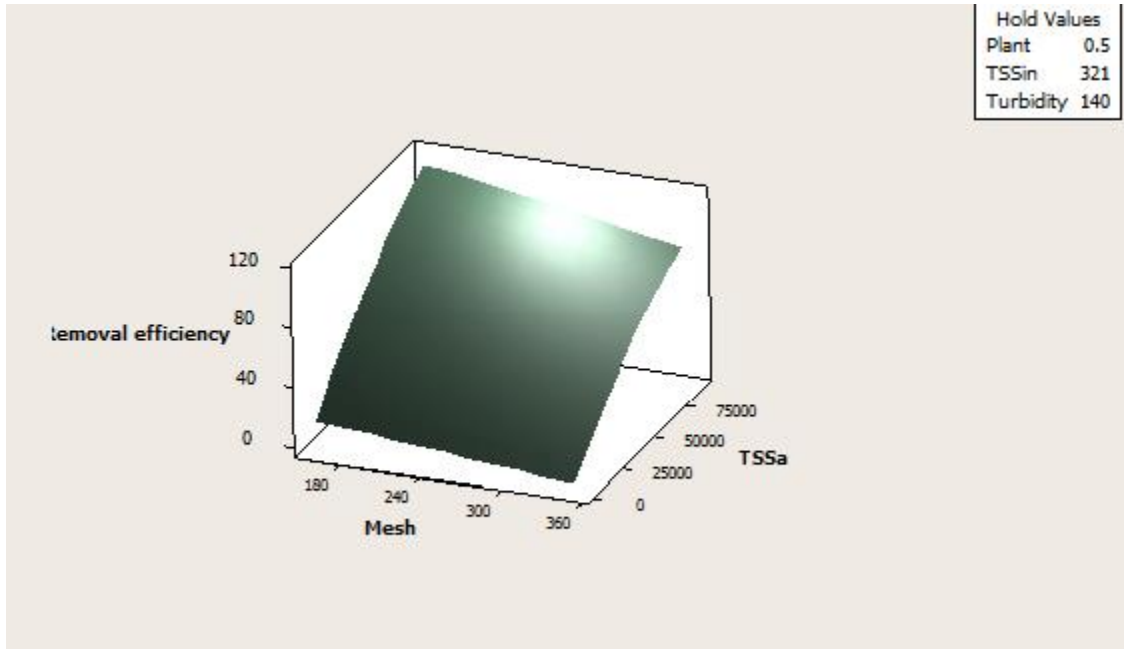


Fig. 4.25: Surface plot of removal efficiency with TSSa and mesh.

In this analysis the additional variable called plants was introduced to determine the effect of the models. While conducting the ANOVA analysis (Table 4.7), in particular the p-value, for the factor "plant" equals to 0.981 indicating it is not a significant factor. The removal efficiency is not dependent on the type of plant considered. The equation of the hypersurface obtained is:

Removal efficiency

$$= 41.46 + Plant * 0.1429 - Mesh * 0.0643 - TSSin * 0.0106$$

..... (4.5)

Table no. 4.7: ANOVA analysis for removal efficiency.

S = 7.97652	PRESS = 31342.6
R-Sq = 83.12%	R-Sq(pred) = 81.14% R-Sq(adj) = 82.43%

Analysis of Variance for Removal efficiency

Source	DF	Seq SS	Adj SS	Adj MS	F	P
Regression	18	138164	138164	7675.79	120.64	0.000
Linear	5	127868	9253	1850.68	29.09	0.000
Plant	1	870	0	0.04	0.00	0.981
Mesh	1	19418	907	907.18	14.26	0.000
TSSin	1	10379	1	1.06	0.02	0.897
Turbidity	1	16116	63	62.87	0.99	0.321
TSSa	1	81086	5546	5546.29	87.17	0.000
Square	3	5041	698	232.80	3.66	0.013
TSSin*TSSin	1	161	50	50.27	0.79	0.375
Turbidity*Turbidity	1	530	185	185.41	2.91	0.089
TSSa*TSSa	1	4350	401	400.78	6.30	0.012
Interaction	10	5255	5255	525.52	8.26	0.000
Plant*Mesh	1	156	544	544.37	8.56	0.004
Plant*TSSin	1	920	845	844.61	13.27	0.000
Plant*Turbidity	1	98	364	364.39	5.73	0.017
Plant*TSSa	1	327	51	51.00	0.80	0.371
Mesh*TSSin	1	874	53	53.21	0.84	0.361
Mesh*Turbidity	1	931	22	21.83	0.34	0.558
Mesh*TSSa	1	573	275	274.69	4.32	0.038
TSSin*Turbidity	1	799	166	165.91	2.61	0.107
TSSin*TSSa	1	66	350	350.48	5.51	0.019
Turbidity*TSSa	1	513	513	513.09	8.06	0.005
Residual Error	441	28059	28059	63.62		
Total	459	166223				

The most important factors are the mesh and TSS_a while turbidity and TSS_{in} does not seem to be as important.

The quadratic response surface seems to be sufficient to capture the 83% of the total variability (R^2 adjusted =82.4%) which is reasonable. The hypersurface exhibits a strong curvature in the direction of TSS_a (p value 0.012). It seems there is an interaction effect between type of plant and TSS_{in}, which means that each plant has its own characteristic influent TSS, even though the removal efficiency is not dependent on the wastewater plant. The term “hold values” means that the non-important variables were kept constant, while the significant variables were changed to show the response surface.

Analyzing the removal efficiency it is noticed that for an increase in removal efficiency, the mesh needs to be decreased and the TSS_a has to increase while the other factors can be kept constant as they don't affect removal efficiency significantly. This is in accordance with the fact that lower the mesh size, higher the removal efficiency causing higher amount of accumulated solids on the filter mesh. On the quadratic surface the optimum region corresponds to high values of TSS_a and lower mesh size.

For flux analysis, MiniTab could not be used as it works only for linear models. While using it for finding the response surface for flux, the hypersurface was exhibiting high peaks. This was due to the non-linearity of the problem. Non-linearizing the dataset using special functions such as logarithmic, exponential might help finding the response surface better but since the dataset was already treated in this fashion while doing the regression analysis, the regression equation obtained, serves the purpose of determining flux as a function of operating parameters.

Chapter 5

Conclusions:

5.1 Summary of results:

The present research was aimed at formulating the filtration kinetics of different unclarified wastewater streams. To achieve this, a bench scale model was successfully built and experiments were conducted with it. The objective was to predict the flux and the removal efficiency of the filter mesh using minimum operating factors but with a reasonable accuracy. A funneling approach was used to reduce 18 operating parameters finally to 4 parameters (turbidity, mesh, TSS_a and TSS_{in}) using linear regression at the beginning and then reducing it further with non-linear regression.

The models predicted for both flux and removal efficiency through regression analysis were validated and the models were used to predict beyond the experimental range of values. The equations obtained were robust and could be applied over a range of TSS, turbidity, and two different mesh sizes. Response surface models helped in estimating the change in the surface plot due to variability in the parameters of interest. The developed equations can be used to predict filtration performance of a unit with similar specifications and operating conditions for different wastewater plants. Although, characteristics of wastewater change with wastewater plants, filtration performance was not significantly affected with the change in wastewater plant.

5.2 Future work:

The present study revealed certain areas that would be of significant interest for future research.

They are listed as follows:

- The pilot unit needs to be validated with the equations obtained from the bench scale model. This would help in better prediction of the filtration kinetics of the filter for the region the unit is designed for.
- Use of particle size distribution as a parameter for water quality analysis might make the model stronger since particle size in wastewater samples varies with region.
- Building up of a global database with different wastewater qualities for more accurate predictions.

References:

1. Aarts A, Veldhuis M, Neef R, Rietveld L. Predicting fine screen behavior under different water quality conditions. 2014. IWA conference. Amsterdam.
2. Ademoroti CMA. The effects of metabolic toxicants on BOD measurements. *Env. Chem. and toxicology*. 1985. 155. 177-195.
3. Amarasiriwardena D, Siripinyanond A, Banes R. Trace elemental distribution in soil and compost-derived humic acid molecular fractions and colloidal organic matter in municipal wastewater by flow field-flow fractionation-inductively coupled plasma mass spectrometry (flow FFF-ICP-MS). *J. Anal. At. Spectrom.* 2001. 16. 978-86.
4. American Public Health Organization. www.apha.org. Last accessed on 05/07/2015.
5. Arslan I, Balcioglu I, Tuhkanen T, Bahneman D. $\text{H}_2\text{O}_2/\text{UV-C}$ and $\text{Fe}^{2+}/\text{H}_2\text{O}_2/\text{UV-C}$ versus $\text{TiO}_2/\text{UV-A}$ Treatment for Reactive Dye Wastewater. *J of Env. Engg.* 2000. 126(10). 903-11.
6. Astaraee R, Mohammadi T, Kasiri N. Analysis of BSA, dextran and humic acid fouling during microfiltration, experimental and modeling. *Food and Bio products processing*. 2015. 94. 331-41.
7. Babovic V, Abbott MB. Evolution of equation from hydraulic data: Part I—theory. *J of Hydraulic Res.* 1997. 35(3). 1–14.
8. Balocha M, Akunnab J, Kieransc M, Collierd P. Structural analysis of anaerobic granules in a phase separated reactor by electron microscopy. *Bioresource Tech.* 2008. 99(5). 922–29.
9. Batra V, Tewari P. A process for the preparation of inorganic membrane filters for solid–liquid and solid–gas separations. Indian patent applied (2006). Last accessed 08/05/2015.

10. Belfort G Davis R, Zydney A. The behaviour of suspensions and macromolecular solutions in cross flow microfiltration. *J. Membr. Sci.* 1994. 96. 1-58.
11. Belia E, Amerlinck Y, Benedetti L, Johnson B, Sin G, Vanrolleghem P, Gernaey K, Gillot S, Neumann M, Rieger L, Shaw A, Villez K. Wastewater treatment modelling: dealing with uncertainties. *Water Sci. and Tech.* 2009. 60(8). 1929-41.
12. Bessiere Y, Abidine N, Bacchin P. Low fouling conditions in dead-end filtration evidence for a critical filtered volume and interpretation using critical osmotic pressure. *J of Membr. Sci.* 2005. 264(1-2). 37-47.
13. Bettenhausen KD, Marenbach P. Self-organizing modelling of biotechnological batch and fed-batch fermentations. In: *EUROSIM'95*. Vienna, Austria: Elsevier Science Publishers B.V. 1995. 445–50.
14. Broeckmann A, Busch J, Wintgens T, Marquardt W. Modeling of pore blocking and cake layer formation in membrane filtration for wastewater treatment. *Desalination*. 2006. 189(1-3). 97-109.
15. Bourgeois W, Burgess J, Stuetz R. On-line monitoring of wastewater quality- a review. *J of Chem Tech and Biotech.* 2001. 76(4). 337-48.
16. Chi F, Cheng W. Use of Chitosan as Coagulant to Treat Wastewater from Milk Processing Plant. *J Polym Env.* 2006. 14. 411–17.
17. Christensen, G. L. and Dick, R. I. Specific Resistance Measurements: Methods and Procedures. *J of Env. Engr. ASCE.* 1985a. 111(3). 258-271.
18. Christensen, G. L. and Dick, R. I. Specific Resistance Measurements: Nonparabolic Data. *J of Env. Engr. ASCE.* 1985b. 111(3). 243-257.

19. Christy C, Vermant S .The state-of-the-art of filtration in recovery processes for biopharmaceutical production. *Desalination*. 2002. 147 (1-3). 1-4.
20. Chu L, Li. S. Filtration capability and operational characteristics of dynamic membrane bioreactor for municipal wastewater treatment. *Sep. Purif. Tech*. 2006. 51(2). 173–179.
21. Cristóvão R, Botelho C, Martins R, Loureiro J, Boaventura R. Fish canning industry wastewater treatment for water reuse – a case study. *J of Cleaner Production*. 2015. 87. 603-12.
22. Díaz E, Stams A, Amils R, Sanz J. Phenotypic Properties and Microbial Diversity of Methanogenic Granules from a Full-Scale Upflow Anaerobic Sludge Bed Reactor Treating Brewery Wastewater. *Appl. Env. Microbiol*. 2006.72(7). 4942-4949.
23. Duffy J, Warnick JE. Using Symbolic Regression to Infer Strategies from Experimental Data. *Evolutionary computation in economics and finance*. 2002. 100. 61-82.
24. Dunn R, Scamehorn J, Christian S. Concentration Polarization Effects in the Use of Micellar-Enhanced Ultrafiltration to Remove Dissolved Organic Pollutants from Wastewater. *Sep Sci and Tech*. 1987. 22 (2-3). 763-89.
25. Fogel LJ, Owens AJ, Walsh MJ. Artificial intelligence through simulated evolution. New York: Wiley, 1996.
26. Fogelman S, Zhao H, Blumenstein M. A rapid analytical method for predicting the oxygen demand of wastewater. *Anal Bioanal Chem*. 2006.386.1773–79.
27. Georgiou D, Aivazidis A, Hatiras J, Gimouhopoulos K. Treatment of cotton textile wastewater using lime and ferrous sulphate. *Water Res*. 2003. 37(9). 2248-50.
28. Goldberg DE. Genetic algorithms in search, optimization, and machine learning. Reading, MA: Addison-Wesley. 1989.

29. Government of Canada. Statistics Canada. www.statcan.gov.ca. Last accessed on 14/05/2015.
30. Greenkorn, R.A, Dekher M. Flow Phenomena in Porous Media.1982. New York.
31. Guwy A, Farley L, Cunnah P, Hawkes F, Hawkes D, Chase M, Buckland H. An automated instrument for monitoring oxygen demand in polluted water. *Water Res.*1999. 33. 3142-48.
32. Hannouche A, Ghassan C, Ruban G, Tassin B, Lemaire B, Joannis C .Relationship between turbidity and total suspended solids concentration within a combined sewer system.. *Water Sci and Tech.* 2011. 64(12).2445-52.
33. Henze M, Harremoes P, Janjzen J, Arvin E. Wastewater treatment, Biological and chemical processes, 3rd edition.2002. Berlin.
34. Henze M. Biological Wastewater Treatment: Principles Modelling and Design. 2008. ISBN: 9781843391883. IWA Publishing, London, UK.
35. Ho C, Zydney A. A combined pore blockage and cake filtration model for protein fouling during microfiltration. *J. Colloid Interface Sci.* 2000. 232(2). 389–99.
36. Hong Y-S. Evolutionary self-organizing modelling and optimization: the application of a paper coating process. Proceeding of the 2001 Joint Conference of Society of Chemical Engineering N.Z. (SCENZ), Food Engineering Association of N.Z.(FEANZ), Engineering Material Group(EMG), Auckland, New Zealand. 2001. 77–81.
37. Hong Y-S. Self-model-generation modelling for water quality of in-stream in urban watershed. Annual New Zealand Hydrological Society Conference, Napier, New Zealand, 1999.
38. Hoek E, Guiver M, Nikonenko V, Tarabara V, Zydney A. Encyclopedia of Membrane Science and Technology, Wiley, Hoboken, NJ. 2013. 3. 2219–2228

39. Holland JH. *Adaptation in natural and artificial systems*. Michigan: The University of Michigan Press, 1975.
40. Jørgensen M , Keiding K, Christensen M. On the reversibility of cake buildup and compression in a membrane bioreactor. *J of membr. Sci.* 2014(455).152-61.
41. Kadam A, Lade H, Lee D, Govindwar S. Zinc chloride as a coagulant for textile dyes and treatment of generated dye sludge under the solid state fermentation: Hybrid treatment strategy. *Bioresource Tech.* 2015. 176. 38-46.
42. Keijzer M, Babovic V. Dimensionally aware genetic programming. *Gecco'99: Proceedings of the Genetic and Evolutionary Computation Conference*, July 13–17, Orlando, USA, 1999.
43. Koza J. *Genetic programming: on the programming of computers by natural selection*. Cambridge, MA: MIT Press, 1992.
44. Lawrence J, Swerhone G, Leppard G, Araki T, Zhang X, West M, Hitchcock A. Scanning Transmission X-Ray, Laser Scanning, and Transmission Electron Microscopy. Mapping of the Exopolymeric Matrix of Microbial Biofilms. *Appl. Environ. Microbiol.* 2003. 69(9). 5543-5554
45. Li W, Sheng G, Wang Y, Liu X, Xu J, Yu H. Filtration behaviors and biocake formation mechanism of mesh filters used in membrane bioreactors. *Sep and Pur. Tech.* 2011. 81(3). 472-79.
46. Lia J, TAO T, Lib X, Zuo J, Lia T, Lua J, Lia S, Chenc L, Xiac C, Liuc Y, Wangd Y; A spectrophotometric method for determination of chemical oxygen demand using home-made reagents. *Desalination.* 2009. 239(1-3).139-45.
47. Logan T. *Agricultural best management practices for water pollution control: current issues*. *Agriculture, Ecosystems and Environment.* 1993. 46 (1-4). 223-31.

48. Marenbach P, Bettenhausen KD, Freyer S, Nieken U, Rettenmaier H. Data-driven structured modelling of a biotechnological fed-batch fermentation by means of genetic programming. *Proc Inst Mech Eng I*. 1997. 211. 325–32.
49. McKay B, Elsey J, Willis MJ, Barton G. Evolving input–output models of chemical process system using genetic programming. *IFAC 96 World Congress, San Francisco, July, 1996*.
50. McKay B, Willis M, Barton GW. Steady-state modelling of chemical process systems using genetic programming. *Comput Chem Eng*. 1997. 21(9). 981–96.
51. Mesquita I, Matosa L, Duarte F, Maldonado-Hódarc F, Mendesa A, Madeira L. Treatment of azo dye-containing wastewater by a Fenton-like process in a continuous packed-bed reactor filled with activated carbon. *J of Hazardous Materials*. 2012. 237-238. 30–37.
52. Metcalf and Eddy. *Wastewater Engineering: treatment and reuse*. 2002. 4th Edition.
53. Monteagudo J, Ortiz M. Removal of inorganic mercury from mine waste water by ion exchange. *J of chemical tech*. 2000. 75(9). 767–772.
54. Perry, RH, Green, DW. *Perry's Chemical Engineers' Handbook*, 8th Edn. McGraw-Hill Professional, New York. 2007. 2072-2100.
55. Pena M, Coca M, Gonzalez G, Rioja R, Garcia M. Chemical oxidation of wastewater from molasses fermentation with ozone. *Chemosphere*. 2003. 51(9). 893-900.
56. Petsev D, Starov V, Ivanov I. Concentrated dispersions of charged colloidal particles: sedimentation, ultrafiltration and diffusion. *Colloids and Surf. A*. 1993. 81. 65-81.
57. Poch M, Comas J, Roda I, Marre M, Coertes U. Designing and building real environmental decision support systems. *Env. Mod. and Soft*. 2004. 19. 857-73.

58. Pulido J, Verardod V, Carretero A, Fereza A. Analysis of the concentration polarization and fouling dynamic resistances under reverse osmosis membrane treatment of olive mill wastewater. *J of Industrial and Eng. Chemistry*. 2015. In press.
59. Qina Z, Lianga Y, Liua Z, Jianga W. Preparation of InYO_3 catalyst and its application in photodegradation of molasses fermentation wastewater. *J of Env Sciences*. 2011. 23(7). 1219–122.
60. Rakib S, Sghyar M, Rafiq , Larbot A, Cot L. New porous ceramics for tangential filtration. *Sep. and Pur. Tech*. 2001. 25. 385–390.
61. Rechenberg I. *Evolutionsstrategie—optimierung technischer.systeme nach prinzipien der biologischen evolution*. Stuttgart: Frommann-Holzboog. 1973.
62. Saboya L, Maubois J. Current developments of microfiltration tech. in dairy industry. *Dairy Sci and Tech*. 2000. 80 (6). 541-53.
63. Saffaj N, Younsi S, Albizane A, Messouadi A, Bouhria M, Persin M, Cretin M, Larbot A. Elaboration and properties of $\text{TiO}_2\text{-ZnAl}_2\text{O}_4$ ultrafiltration membranes deposited on cordierite support. *Sep. and Pur. Tech*. 2004. 36. 107–114.
64. Saffaj N, Younsi S, Albizane A, Messouadi A, Bouhria M, Persin M, Cretin M, Larbot A. Processing and characterization of $\text{TiO}_2/\text{ZnAl}_2\text{O}_4$ ultrafiltration membranes deposited on tubular support prepared from Moroccan clay. *Ceram. Int*. 2005. 31. 205–210
65. Sánchez-Martína J, Beltrán-Herediaa J, Delgado-Regañaa A , Rodríguez-Gonzálezb M, Rubio-Alonsoc F. Optimization of tannin rigid foam as adsorbents for wastewater treatment. *Industrial Crops and Products*. 2013. 49. 507–514.
66. Sarkar B, Chakrabarti P, Vijaykumar A, Kale V. Wastewater treatment in dairy industries- possibility of reuse. *Desalination*. 2006. 195(1-3). 141-152.

67. Satyawali Y, Balakrishnan M. Wastewater treatment in molasses-based alcohol distilleries for COD and color removal – a review. *J of Env. Mang.* 2008. 86(3). 481-97.
68. Seo G, Moon B, Park Y, Kim S. Filtration characteristics of immersed coarse pore filters in an activated sludge system for domestic wastewater reclamation. *Water Sci. Tech.* 2007. 55. 51–58.
69. Solpan D, Guven O, Takacs E, Wojnarovits L, Dajka K. High-energy irradiation treatment of aqueous solutions of azo dyes: steady-state gamma radiolysis experiments. *Radiation Phy. and Chem.* 2003. 67(3-4). 531-34.
70. Tewari P, Singh R, Batra V, Balakrishnan M. Membrane bioreactor (MBR) for wastewater treatment: Filtration performance evaluation of low cost polymeric and ceramic membranes.. *Sep. and Pur. Tech.* 2010. 71(2). 200-04.
71. Tien C. *Introduction to Cake Filtration: Analyses, Experiments and Applications.* 2006.
72. Vesilind, P. A. *Treatment and Disposal of Wastewater Sludges,* 1979, Ann Arbor, MI.
73. Wang Q, Matsuura T, Feng C, Weir M, Detellier C, Rutadinka E, Van Mao R. The sepiolite membrane for ultrafiltration. *J. Membr. Sci.* 2001. 184(2). 153–163.
74. Wells' S, Dick R. synchrotron radiation evaluation of gravity sedimentation effects prior to dewatering. *ASCE-CSCE national conference on environ. Eng. Vancouver. BC.* 845-52.
75. Wu Y, Huang X, Zuo W. .Effect of mesh pore size on performance of a self-forming dynamic membrane coupled bioreactor for domestic wastewater treatment. 5th International Membrane Science and Technology conference, Sydney, November 11–13 (2003).
76. Wu Y, Huang X, Zuo W. Effect of mesh pore size on performance of self-forming dynamic membrane coupled bioreactor for domestic wastewater treatment, future of urban

wastewater systems—decentralization and reuse. IWA International Conference, Xi'an China, May 18–20 (2005).

77. Zhou F, Husain H. Use of Chemical Coagulants to Control Fouling Potential for Wastewater Membrane Bioreactor Processes. *Water Environ. Res.* 2007. 79(9). 952-57.
78. Whigham PA, Craper PF. Time series modelling using genetic programming: an application to rainfall-runoff modelling. In: Spector L, Langdon WB, O'Reilly U, Angeline PJ, editors. *Advances in genetic programming 3*, Cambridge, MA, USA: MIT Press. 1999. 5. 89–104.
79. Willis M, Hiden H, Hinchliffe M, McKay B, Barton GW. Systems modelling using genetic programming. *Computers & Chemical Engineering* 1997. 21. 1161–66.

Appendix:

SAS Coding:

```
proc import datafile = 'tu.csv' out=correct2 replace;
  guessingrows = 1000;

run;

ods html exclude all;

proc reg;

  model Flux=TSSa Mesh TSSin l1c l2c l3c l4c SV11350 SV12350 SV13350
SV14350 SV11158 SV12158 SV13158 SV14158 Turbidity350 Turbidity158
SVturb158 SVturb350 SVTCOD350 SVTCOD158 TCOD350 TCOD158 TSSSVout SVEff350
SvEff158

  /selection = cp AIC sbc;

  ods output subsetsselsummary=models;

run;

ods html select all;

proc sort;

  by AIC;

run;

proc print data=models( obs=10);

title 'Best 10 models by AIC';

run;

proc sort;

  by sbc;

run;
```

```

proc print data=models( obs=10);
title 'Best 10 models by BIC';
run;

proc import datafile = 'tu.csv' out=correct2 replace;
  guessingrows = 1000;
run;

proc reg;

model Flux=TSSa Mesh TSSin l1c l2c l3c l4c SV11350 SV12350 SV13350 SV14350
SV11158 SV12158 SV13158 SV14158 Turbidity350 Turbidity158 SVturb158
SVturb350 SVTCOD350 SVTCOD158 TCOD350 TCOD158 TSSSVout SVEff350 SvEff158
  /selection = cp AIC sbc best = 10;

title 'Cp model selection';

run;

proc glm;

model Flux=TSSa Mesh TSSin l1c l2c l3c l4c SV11350 SV12350 SV13350
SV14350 SV11158 SV12158 SV13158 SV14158 Turbidity350 Turbidity158
SVturb158 SVturb350 SVTCOD350 SVTCOD158 TCOD350 TCOD158 TSSSVout SVEff350
SvEff158;

title 'Regression of log brain size on log body, log litter and log
gest';

run;

proc sgscatter;

matrix Flux TSSa Mesh TSSin l1c l2c l3c l4c SV11350 SV12350 SV13350
SV14350 SV11158 SV12158 SV13158 SV14158 Turbidity350 Turbidity158

```


Date	Time	Plant	Sample	Mesh	TSSin (mg/l)	TSSout (mg/l)	Turbidity (NTU)	Permeability	TSSa (mg/m2)	Removal efficiency
20th May, 2015	8.25 AM	Adelaide	Control 1	350	167	167	77	1420	0	
			350-1-1	350	167	147	77	715.5895184	4933.885929	11.9760479
			350-1-2	350	167	110	77	555.9754328	14253.99645	35.34805389
			350-1-3	350	167	105	77	339.6497741	18936.25419	43.71257485
			350-1-4	350	167	94	77	188.7622294	32356.42392	50.89820359
			Control 3	350	221	221	67	1420	0	
			350-3-1	350	221	114	67	490.4927053	49013.22281	48.85894157
			350-3-2	350	221	108	67	402.0191851	61609.43359	50.22624434
			350-3-3	350	221	110	67	316.8304284	70529.89935	51.13122172
			350-3-4	350	221	108	67	108.0267121	90393.7241	55.20361991
			Control 4	350	141	141	69	1420	0	
			350-4-1	350	141	118	69	604.2375814	8658.969805	17.78115502
			350-4-2	350	141	113	69	507.5425471	11722.91297	19.14893617
			350-4-3	350	141	114	69	363.7979306	14096.1121	26.24113475
			350-4-4	350	141	104	69	222.677265	21585.75094	32.62411348
			Control 5	350	184	184	78	1420	0	
			350-5-1	350	184	137	78	555.2740664	11826.35001	25.54347826
			350-5-2	350	184	120	78	507.3472804	18141.63078	34.7826087
			350-5-3	350	184	102	78	196.6653624	27851.37497	44.56521739
			350-5-4	350	184	68	78	172.1240096	38725.49905	63.04347826

Eureqa snapshots:



Enter Data



Prepare Data



Define Search



Start Search

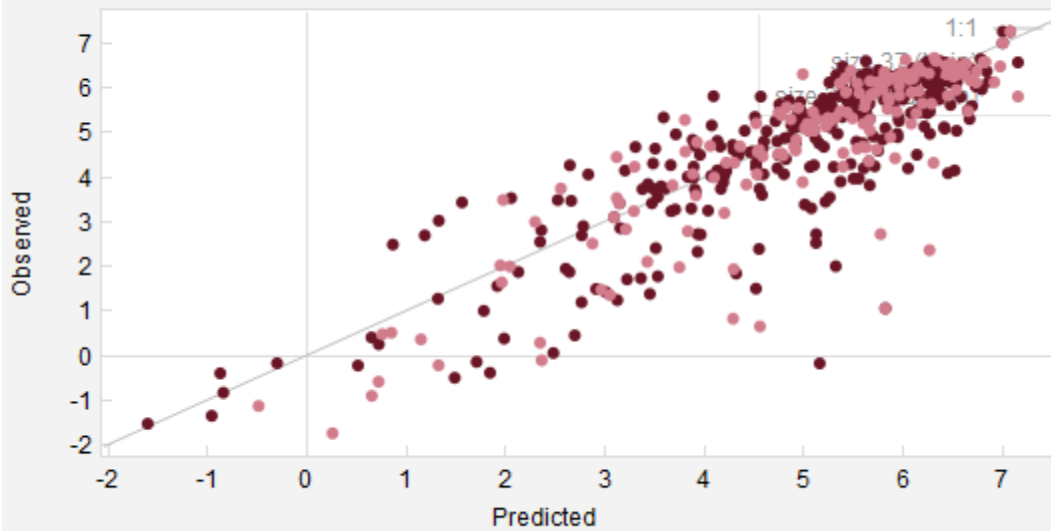


Results

Best Solutions of Different Sizes

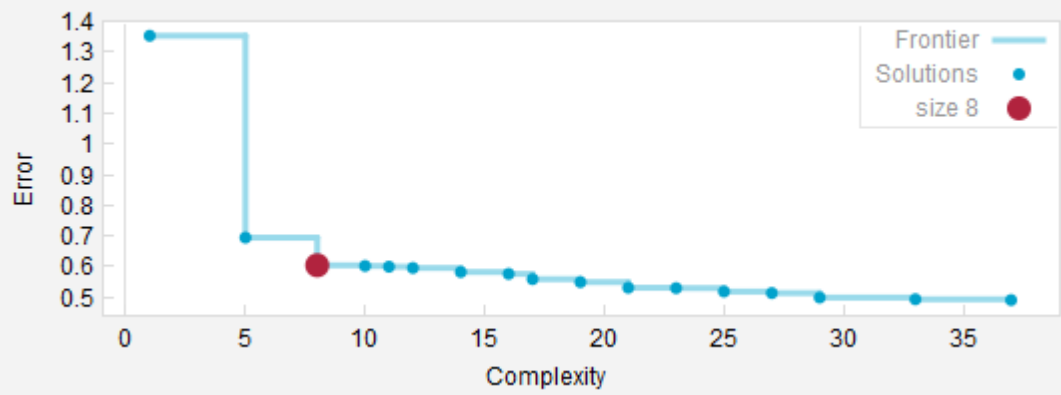
Size	Fit	Solution
8	0.447	$d = 7 + \frac{-18.5e}{a}$
21	0.392	$d = 6.58 + 0.00215b + 0.000284ae - 0.107e - 0.000477ce$
17	0.413	$d = 7.01 + 0.000242ae - 0.107e - 0.000348ce$
10	0.445	$d = 7 + \frac{-22.3e}{41.4 + a}$
19	0.406	$d = 7 + 0.000428ae - 0.162e - 1.17e-6ace$
11	0.443	$d = 7 + 0.000277ae - 0.156e$
14	0.430	$d = 6.79 + 0.00133a + \frac{-34.2e}{148 + a}$

Plot Type:



XAxis:

Solutions Plotted Accuracy vs Complexity



Solution Details (calculated on validation data)

Solution	$d = 6.942 + 0.0003878*a + 0.0009893*b*e + 0.000256*a*e - 0.2581*e - 3.839e-6*b*c*e - 4.218e-6*c*e^2$
R^2 Goodness of Fit	0.79705652
Correlation Coefficient	0.90148868
Maximum Error	4.7617114
Mean Squared Error	0.72673507

Curriculum vitae:

Name: Tulip Chakraborty

Post-Secondary Education and Heritage Institute of Technology

Degrees: Kolkata, West Bengal, India

B.Tech Biotechnology

2009 – 2013

The University of Western Ontario

London, Ontario, Canada

M.E.Sc. Chemical and Biochemical Engineering

2013 – 2015

Honors and Awards: Western Graduate Research Scholarship (2013 – 2015)

Mitacs Scholarship (January – June 2015)

Second place at Sarnia – Western Conference (July 2015)

Related Work Experience: Graduate Teaching Assistant

The University of Western Ontario

January – April 2013

Research Intern

Trojan Technologies

June 2014 – June 2015